

**CHARACTERIZATION OF THIN-BEDDED RESERVOIR IN THE
GULF OF MEXICO: AN INTEGRATED APPROACH**

A Thesis

by

SEVERINE LALANDE

Submitted to the Office of Graduate Studies of
Texas A&M University
in partial fulfillment of the requirements for the degree of

MASTER OF SCIENCE

May 2002

Major Subject: Geophysics

**CHARACTERIZATION OF THIN-BEDDED RESERVOIR IN THE
GULF OF MEXICO: AN INTEGRATED APPROACH**

A Thesis

by

SEVERINE LALANDE

Submitted to Texas A&M University
in partial fulfillment of the requirements
for the degree of

MASTER OF SCIENCE

Approved as to style and content by:

Joel S. Watkins

(Co-Chair of Committee)

Wayne M. Ahr

(Co-Chair of Committee)

Duane McVay

(Member)

Andrew Hajash, Jr.

(Head of Department)

May 2002

Major Subject: Geophysics

ABSTRACT

Characterization of Thin-Bedded Reservoir in the Gulf of Mexico:

An Integrated Approach. (May 2002)

Séverine Lalande, B.S., Ecole Nationale Supérieure des Mines de Paris

Co-Chairs of Advisory Committee: Dr Joel S. Watkins
Dr Wayne M. Ahr

An important fraction of the reservoirs in the Outer Continental Shelf of the Gulf of Mexico is comprised of thin-bedded deposits from channel-levee systems. These reservoirs are particularly difficult to describe. Not only is their architecture complex but the quality of the reservoir is determined by connection and length of beds below the resolution of usual reflection data. Improved characterization is needed to improve development and production of these reservoirs. This study presents an integrated approach to build a geologically consistent reservoir model, based on the 8 sand reservoir in Northern Green Canyon block 18. The underlying idea of the construction of this model is that reservoir quality is influenced more by the internal architecture than by the statistical values of petrophysical parameters.

Seismic interpretation and attribute extraction provided the reservoir geometry and stratigraphy. The structural framework and the limits of the reservoir have been determined, showing the preeminent role of salt and faults in the constitution of this reservoir.

Seismic attributes are calibrated to extract areal information on reservoir architecture. Gross thickness and net thickness maps have been estimated using geostatistical methods. Lateral variations in the quality of the 8 sand and the definition zones with different average properties were inferred from geostatistical results.

Lithofacies characterization from cores showed that 3 facies could be used to describe the internal variability. The fine-scale heterogeneity is described in each zone from vertical facies distribution determined from wells.

A truncated Gaussian sequential simulation was performed to reflect both the regional trend and the internal variability on a 150*150*1 ft grid.

The major contribution of this work is to show the efficiency of this approach to describe complex reservoirs where the impact of internal variability is a major control of flow efficiency. This is especially valuable when the well information is scarce or not uniformly distributed. This model will be used for flow simulation and sensitivity analysis to improve the field description.

ACKNOWLEDGEMENTS

I am most grateful to my committee members for their guidance and support. I thank Dr Joel Watkins for serving as the chairman of my thesis committee, I am also appreciative of the efforts and commitment of Dr Wayne Ahr, as a co-chair, and Dr Duane McVay, as committee member. They made it possible to conduct this research as a real integrated project.

I thank Burlington Resources for providing the data for this study and Lee Williams for gathering the data set.

I acknowledge all students who provided technical assistance in my study particularly Rasheed Jaradat who helped me with IESX utilization and provided very helpful comments during this research.

I also would like to thank all the friends who supported and encouraged me during these months.

TABLE OF CONTENTS

	Page
ABSTRACT	iii
ACKNOWLEDGEMENTS	v
TABLE OF CONTENTS	vi
LIST OF FIGURES	viii
LIST OF TABLES	xii
 CHAPTER	
I INTRODUCTION.....	1
Location.....	1
Database	3
Objectives.....	3
II BACKGROUND.....	5
Deposits in turbidite systems.....	5
Salt tectonic influence	8
Generalized stratigraphic models	9
III METHODS.....	13
Structural mapping	13
Reservoir delineation.....	13
Seismic attributes	19
Data integration using geostatistics.....	22

CHAPTER	Page
IV RESULTS.....	28
Structure and stratigraphy.....	28
Geological information from seismic.....	34
Geostatistical model	40
V DISCUSSION AND SUMMARY	48
Reservoir structure	48
Depositional environment	48
Guidelines for reservoir modeling.....	49
Summary	50
REFERENCES CITED	51
VITA	58

LIST OF FIGURES

FIGURE	Page
1. Green Canyon cumulative productions from 1987 to 1999	2
2. Northern Gulf of Mexico map showing the outer continental shelf leasing areas. GC-Green Canyon. The star indicates the location of block GC-18.....	4
3. Shot point plot for GC-18 seismic survey. Well paths are projected showing location and deviation.	4
4. Conceptual model of a mud-rich turbiditic system, with the main architectural elements. Modified from Reading and Richard (1994).....	6
5. Structure contour map of top salt or equivalent salt weld in Northern Green Canyon. Shows shallow salt bodies in black (<3.0s TWT), thin salt in gray (>3.0s TWT) and salt weld in white (<100 ms thick). Square indicates block GC 18. From Mc Bride et al. (1998).....	8
6. Interpreted sediment pathway in Northern Green Canyon for 1.4-1.9 Ma sequence. Square indicates block GC 18. From Weimer et al. (1998b).). Shaded gray zones represent paleo-highs associated with salt.....	9
7. Sequence stratigraphic model showing idealized development of systems tracts in an expanded Late Cenozoic section for the Northern Gulf of Mexico. From Mitchum et al. (1993).	11
8. Generalized model for sequence stratigraphy showing relationships between salt tectonism, growth faulting and distribution of system tracts. From Zhang (1994).	11
9. Raw and interpreted crossline 3170 shows high amplitude reflection associated to salt limits and major fault.	14
10. Check-shot data in GC 18..	15

FIGURE	Page
11. Composite display of well log curves, synthetic and seismic showing correlation of top 8 sand from well to seismic.	17
12. Amplitude map of the top of the reservoir showing low amplitudes (red) in the southwest part related to variable quality of the reflector and elongated low amplitude trend in the northwest interpreted as discontinuities in the reservoir. ...	20
13. Scatter plots of seismic attribute (energy half time) versus gross and net thickness measured at wells.	21
14. (a) Omnidirectional variograms of the gross thickness from well information only. (b) Variogram of reservoir isochron derived from seismic, D1 is the X axis, D2 the Y axis. Thin lines are experimental variograms, bold lines are models. The dotted line indicates the variance of the data.....	25
15. Principle of computation of proportions curves. The relative proportion of facies is characterized vertically from well data. (Modified from Doligez et al., 1999).	27
16. Structure map of the top of the salt ridge	29
17. Salt isopach, two salt bodies separated by a thinner zone in red <100 ms.....	29
18. Coherence slice at 3176 ms (intersects the reservoir) showing some fault traces and origin of the diapir in the southeast	30
19. Interpreted section showing salt ridge and major faults intersecting the reservoir. Orange horizon is top of sand 8.	31
20. Time structure of the top of the 8 sand reservoir with trace of major faults.....	31
21. Depth structure of the top of the reservoir.	32
22. Seismic derived isopach between the top of the reservoir and the top of the CM sequence (1.4 Ma) indicating beginning of salt withdrawal early after deposition.	33

FIGURE	Page
23. Cosine of phase display of a section enhancing the continuity of the reflector. It shows the shingled pattern of 8 sand and overlapping of the eastern reflectors.....	34
24. a) Thickness map derived from well data only and b) its associated variance of estimation. Away from the wells the uniform value shows the lack of information.....	35
25. Seismic-derived isopach of the 8 sand reservoir.....	36
26. a) Thickness map incorporating seismic and well information and b) associated variance of estimation, much reduced compared to the case with well information only Figure 24.....	37
27. Map of the seismic attribute (energy half time) used to derive the drift of net thickness.....	38
28. Net pay map incorporating well and seismic attribute information. The arrow shows an anomaly where the net thickness is equal to the gross thickness.	39
29. Zonation of the reservoir based on net thickness and facies proportion at wells. Zone I and II have an average net-to-gross of 45%. Zone I delineates the main flowpath where channel facies are more continuous. Zone I is the most distal part with an average net-to-gross of 39%. Faults are not taken into account.....	41
30. Vertical proportion curves generated from facies identified at wells gathered by zones to respect lateral variation in average facies proportions (Zone III with higher proportion of facies E) and vertical associations (Zone I with a continuous interval of facies A whereas they are more scattered in the upper part in zone II).	42
31. 3D lithofacies simulation of the 8sand on a 150*150*1ft grid with a lateral range of 850ft and a vertical range of 10 ft. Within each unit the lateral continuity is good but the vertical continuity varies..	44

FIGURE	Page
32. N-S section of the 8 sand lithofacies simulation. The separation in zones enables to represent the lateral variations in average net-to-gross. The location map shows in red the simulated section and in blue the well section of Figure 33. Vertical lines represent the projection of well location.....	45
33. Well correlation of the 8 sand from Plantevin 2002. The location map shows in blue the well section and in red the simulated section of Figure 32..	46

LIST OF TABLES

TABLE	Page
1. Correlation coefficients between seismic attributes and well properties. The correlation is generally non significant except for net thickness, gross thickness and energy half time (abbreviated e-half).	21
2. Comparison of geostatistical estimation techniques. From Isaaks and Srivastava (1989), Hohn (1999), Doyen (1996), Xu et al., (1992).	24

CHAPTER I

INTRODUCTION

An increasing share of new discoveries has been found in deep marine environments. These fields present very complex reservoir architecture related to the spatial arrangement of sand bodies and internal variability (Sheibal et al. 1992). Their characterization is challenging as the typical scale of heterogeneities is near or below the resolution of seismic reflection data.

The complex internal architecture of these stacked turbidite reservoirs motivated an integrated approach to build a realistic model for one of Green Canyon 18's reservoirs. Geostatistical methods were applied to synthesize geological and geophysical interpretations.

LOCATION

Green Canyon 18 (GC18) is a 5888 acres block located 113 km (70 miles) offshore Louisiana, south of Morgan City in 232 m (760 ft) water depth (Brinkmann et al., 1987). The field was discovered in 1982; as of Dec 2001 it was jointly own by Exxon Mobil (55% working interest), BHP (25% WI), Burlington (15% WI) and Kerr McGee (5% WI) (Weimer et al., 1998a). The oil has 28 API gravity.

Producing intervals range from middle Pliocene to Pleistocene. Sixteen different reservoir intervals have been completed between 2211 m and 4571 m (6700 ft and 13850 ft). The oldest pay (MP2-MP3) belong to the 3.8-3 Ma sequence and is produced in the northern part of the prospect, in the south of Ewing Banks block 988.

The main pay consists of the “numbered sands”, 8 to 30, which are part of a turbidite package in the 1.4-1.9 Ma sequence generally referred as the Calcidiscus

This thesis follows the style and format of the *Bulletin of the American Association of Petroleum Geologists*.

Macintyre sequence. The younger reservoirs (Trim A and Trim B) in the Trimosina sequence (0.8-0.3 Ma) are middle Pleistocene. Producing operations started in May 1987. As of October 1999, Green Canyon 18 reservoirs had produced 70 MMSTB of oil and 88 Bcf of gas. Figure 1 shows the evolution of cumulative production.

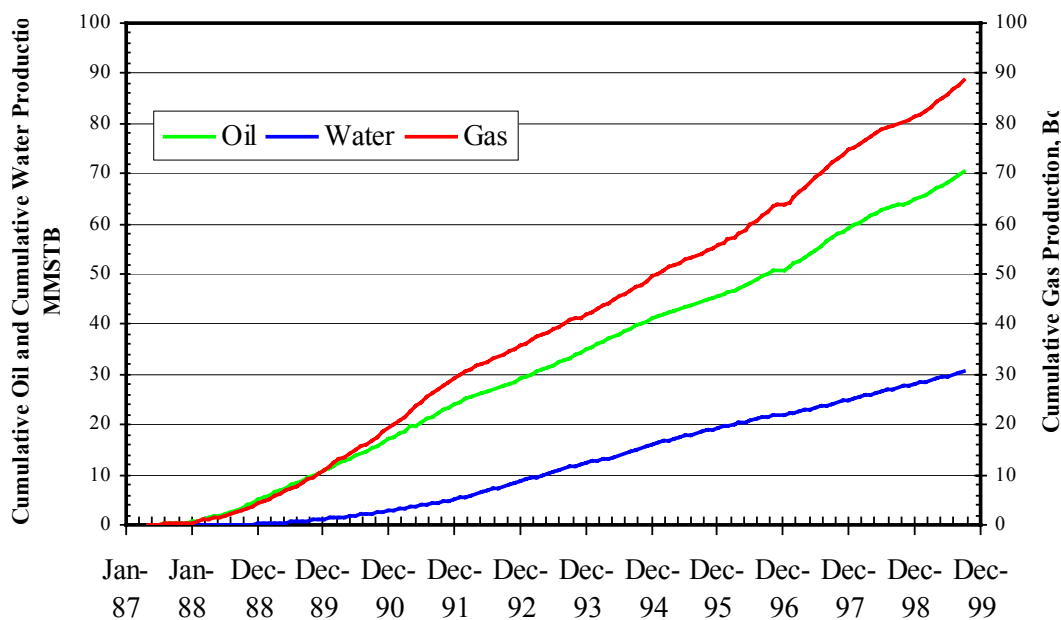


Figure 1. Green Canyon cumulative productions from 1987 to 1999.

The problems encountered in this field are related to the complex structure and the difficulties of correlation of the sand bodies. The extension/connectivity of the reservoirs remain uncertain after two 3D surveys. Risks are increased by overpressure and compaction related problems. Green Canyon 18 has produced from 32 wells (49 completion intervals) and has experienced many well failures leading to the premature loss of 50% of all producing intervals (Tackett W. M. pers. com. Aug 1998).

Improving development of this type of reservoir requires a better understanding of flow parameters and requires construction of a realistic geological model integrating all static data.

DATABASE

The data set (see Figure 2 for geographical location) consists of:

- 3D migrated seismic survey from Diamond Geophysical/Burlington with a spacing of line 65.62 ft and of trace 41.01 ft, covering the 3*3 sq. mi. block.
- 48 wells and deviation data (see Figure 3).
- 19 check shot surveys.

OBJECTIVES

This research focuses on the upper sand of the numbered interval: Sand 8. The overall purpose of this study is to gain an understanding of this reservoir, integrating geological and geophysical aspects in order to provide a geological model and guidelines for flow simulation. The specific objectives are:

- Generate reservoir structure maps.
- Identify reservoir compartments on the basis of depositional and structural characteristics.
- Identify key heterogeneities.

Specifically, this involves:

- Structural and stratigraphic mapping.
- Correlating 8 sand.
- Integrating seismic and geological information using geostatistical tools to provide a quantitative representation of reservoir variability.

CHAPTER II

BACKGROUND

In order to develop a model at the reservoir scale it is important to keep in mind the properties of the parent depositional system. The geologic history of this area is complex owing to a combination of high sedimentation rates, slope instability and salt-related tectonism. The objective of this chapter is to describe the facies encountered in turbiditic systems, to present the influence of salt tectonics on these systems in the Northern Gulf of Mexico Outer Continental Shelf and to review the main stratigraphic models developed in this region to improve reservoir definition.

DEPOSITS IN TURBIDITE SYSTEMS

The deepwater Gulf of Mexico has been an active exploration area for more than 30 years (Iledare, 2000; Kumins, 2000). The principal reservoirs consist of Neogene turbidite systems. A “turbidite system” as described by Mutti and Normark (1987) or “fan lobe” according to Bouma et al., (1985) represents deposition by gravity flow into a basin. These deepwater depositional systems are characterized by a great variability in size, facies, facies association and geometry of sand bodies. One of the causes lies in the nature of the transportation system. Reading and Richards (1994) pointed out that the primary controls of gravity flows are the dominant grain size and the volume of sediment. These influence the extension of the system and the facies organization. According to Bouma et al. (1985), three zones are generally distinguished to describe turbidite systems: the upper fan (on the slope), the middle fan and the lower fan (on the basin floor).

Figure 4 presents a conceptual model of a system analog to those encountered in the Gulf of Mexico called a high-efficiency transportation system and characterized primarily by fine-grained sediments (Reading and Richard, 1994). This model enables the identification of the principal architectural elements of the system.

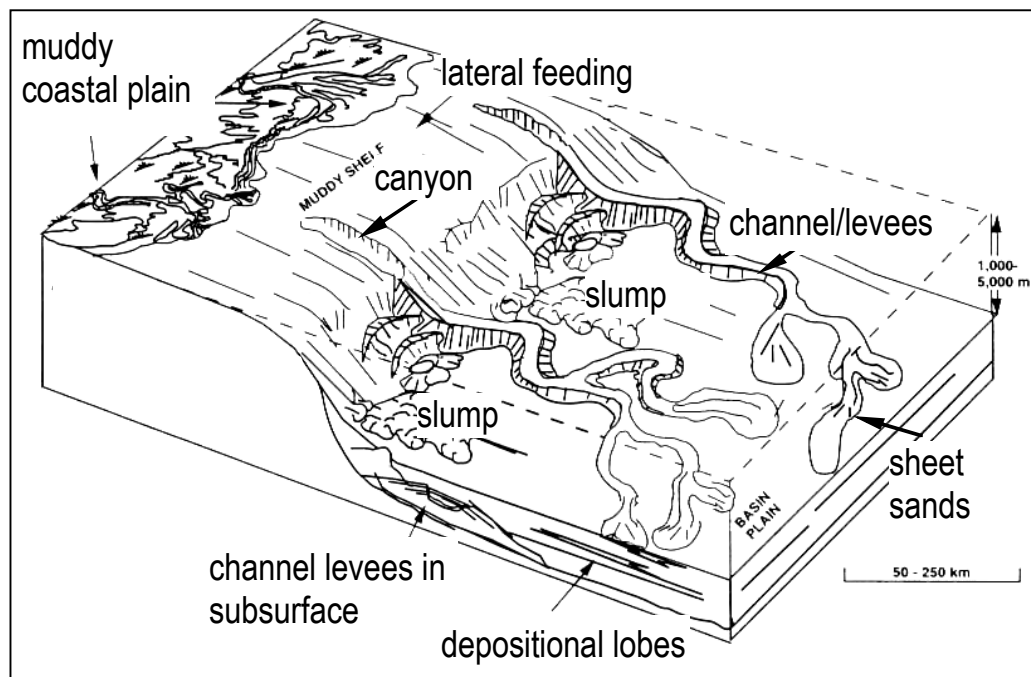


Figure 4. Conceptual model of a mud-rich turbiditic system, with the main architectural elements. Modified from Reading and Richard (1994).

The major erosional feature that incises the slope is the feeder canyon, which controls the flow from the shelf to the basin. At the base of the slope, the change of gradient induces the beginning of the deposition. On the basin floor, the sedimentation is organized in sinuous channel systems flanked by levees made of accumulation of material that spills over the edges during time of high depositional rate. Channels are defined as long-lived sediment pathways, which are both erosional and depositional features. These adjectives are also used to describe their later filling (Varnai 1998). Channels are said erosional when they are filled by shale. Other channels filled by sand exhibit blocky or fining upward log signatures reflecting the thinning of grain size. On seismic, channels may be detected by elongated high amplitude anomalies. Levee deposits reflect a change in the process of deposition from turbulent flow to traction, which efficiently winnows sand (Bouma 2000). It results in fine-grained laminated sands and can show the best porosity-permeability combination in the system. Net-to-gross

sand varies from 30-50% in the proximal levees to 10% in the distal part (Weimer et al., 1998b). Overbank refers to the high shale/sand ratio intervals of the levees. This facies is commonly called “low pay, low resistivity sands” (Darling and Sneider 1992), the log response is highly variable. It is generally described as “nervous” or “ratty”. Wireline tools usually average over several layers. In levees, as the sand/shale laminations are of the order of a few inches they do not enable a correct interpretation of reservoir properties. Thin-bedded sand logs exhibit high gamma ray, low resistivity and high apparent water saturation. On seismic sections, channel-levee systems are characterized by irregular and discontinuous reflection and low to moderate amplitudes without dominant pattern (Pacht and Bowen 1990).

As the system progresses on the basin floor, the channels become narrower, the current is no longer contained and silt begins to spread out into depositional lobes or sheet sands. Although it is believed that only one distributary channel is active at a time, sheet sands are generally stacked and their individual thickness is difficult to assess. Lobes may be separated by amalgamated hemipelagic shales deposited during intervals when no sedimentation occurs in this zone. Log response of sheet sand is generally blocky, reflecting the homogeneity of the sediments. On the seismic they sometimes appear as mounded shapes in cross-section (Armentrout et al., 1995; Mitchum et al., 1993).

Turbidite complexes consist of assemblages of individual turbidites systems. Stacking occurs both vertically and laterally and influences greatly the continuity of the sand bodies.

SALT TECTONIC INFLUENCE

One peculiarity of the Gulf of Mexico is the intense tectonic activity during deposition. Salt movements and growth faults displacements greatly influence the structural development and the depositional pattern.

Many studies have been conducted to decipher the complex relation between salt movement, growth faulting and sediment loading (Karlo and Shoup 2000, Zhang 1994, McBride et al., 1998).

Salt influences stratigraphy in different ways. First salt deformation through time influences the location of mini-basins and thereby controls location of deposition. At depositional time, shallow salt modifies the paleobathymetry and influences flow pathway. Last, salt withdrawal provides accommodation space.

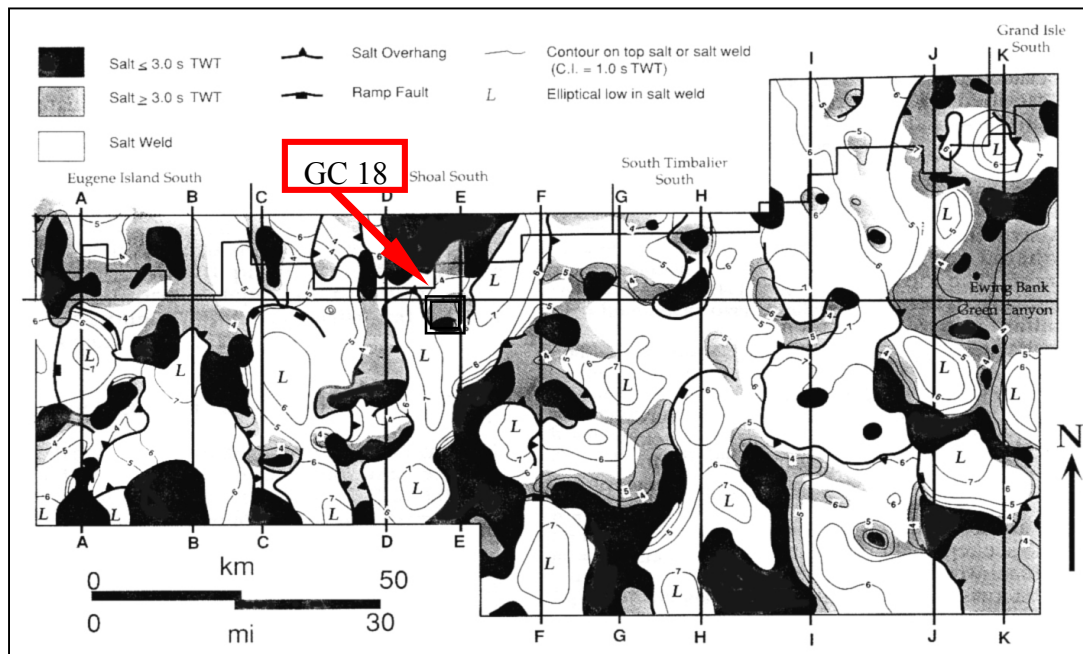


Figure 5. Structure contour map of top salt or equivalent salt weld in Northern Green Canyon. Shows shallow salt bodies in black (<3.0 s TWT), thin salt in gray (>3.0 s TWT) and salt weld in white (<100 ms thick). Square indicates block GC 18. From McBride et al. (1998).

Figure 5, from Mc Bride et al., (1998), shows the contour of salt in the Northern Gulf of Mexico. This area exhibits high salt relief, diapirs are found at the edge of shallow sheets or at the saddle between elliptical lows.

The environment of deposition of the turbidite system is greatly influenced by salt, Figure 6 (from Weimer et al., 1998b) shows a reconstitution of the flow path in the same area during the 1.4-1.9 Ma sequence. The main sediment fairways are located in the center of mini-basins. This map also indicates that basin floor fan deposits are mainly deposited southern of the study area. The prevalent facies in Northern Green Canyon is channel levee systems.

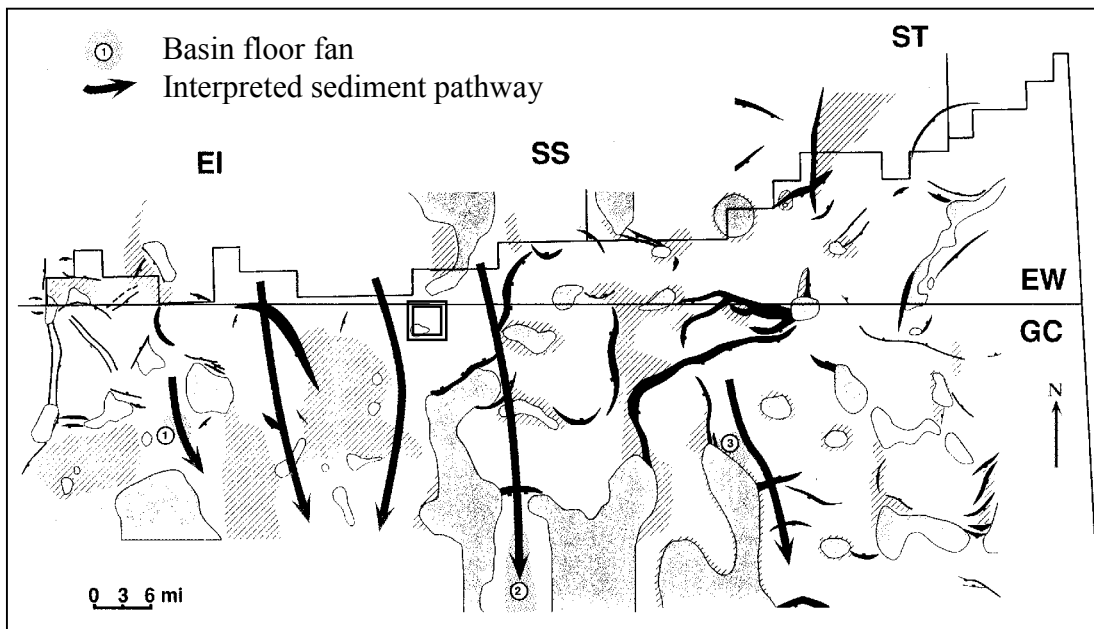


Figure 6. Interpreted sediment pathway in Northern Green Canyon for 1.4-1.9 Ma sequence. Square indicates block GC 18. From Weimer et al. (1998b). Shaded gray zones represent paleo-highs associated with salt.

GENERALIZED STRATIGRAPHIC MODELS

The construction of a general stratigraphic model has attracted the interest of many authors. Several regional studies integrating seismic stratigraphy and paleo-data have helped to understand major depositional controls and their impacts on petroleum

exploration (Mann et al., 1987, Weimer et al., 1998c, Zhang 1994). Turbiditic sedimentation occurs mainly during sea level falls and lowstand periods. When the sea level is high, river sediments are trapped along the inner shelf. When the sea level is low, river sediments are deposited along the outer shelf. They are unstable and can easily create turbidity currents (Bouma et al., 1985).

Mitchum et al. (1993) proposes a model that integrates growth faulting. It emphasises the accommodation provided on the downthrown side of the fault (see Figure 7). Zhang (1994) integrates the salt structure in an environment characterised by intraslope basin separated by salt diapirs. He distinguishes two elements in the lowstand system tract: the basal unit is called “lowstand intrasalt basinal fan” and correspond to deposition when the area is a slope environment. The upper unit called the lowstand wedge is mainly composed of channel levees, see Figure 8. Prather et al. (1998) emphasis the idea of slope accommodation and described a two phases model where upper slope basins are filled first and then bypassed to down dip basins. The first stage deposits are described as “sand-prone ponded basin fill” and the latter as “shale-prone bypass succession”, mainly made of leveed-channel with shallow erosional features.

The relative influence of salt and faults on sedimentation has varied through time. Pliocene sequences are thick and considered to be mainly influenced by salt withdrawal (Weimer et al. 1998c). Conversely, Pleistocene sequences are thinner, show a lower sand/shale ratio and accommodation provided by growth faulting is believed to have been more significant.

Green Canyon 18 producing intervals are representative of these channel-levee systems deposited between shallow salt bodies. The primary reservoirs in Green Canyon 18 are the numbered sands 38 to 8 that occur in the 1,4-1,9 Ma sequence, they are part of a mounded turbidite package. The lower reservoirs 38-18 are interpreted as part of a lower lowstand unit whereas the upper sands belong to the upper lowstand or prograding wedge unit and show smaller sand/shale ratios.

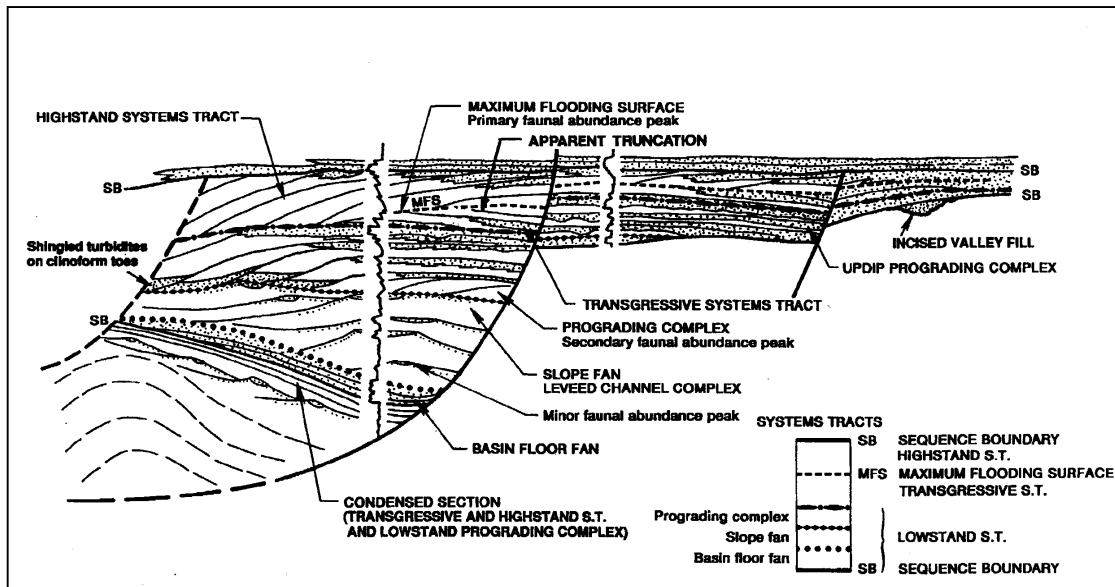


Figure 7. Sequence stratigraphic model showing idealized development of systems tracts in an expanded Late Cenozoic section for the Northern Gulf of Mexico. From Mitchum et al. (1993).

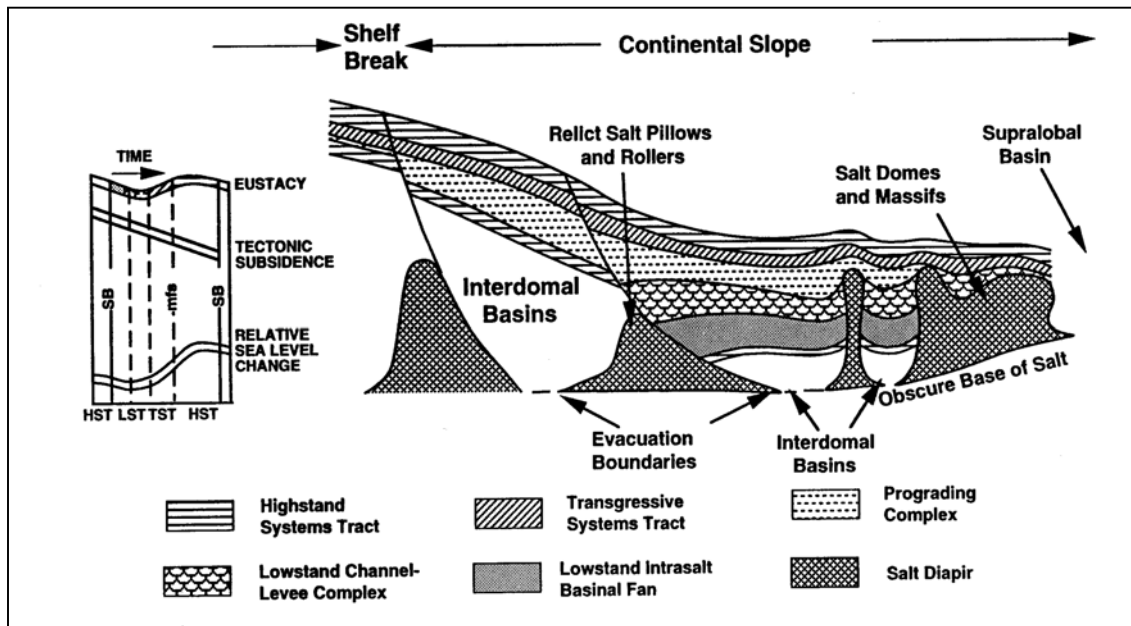


Figure 8. Generalized model for sequence stratigraphy showing relationships between salt tectonism, growth faulting and distribution of system tracts. From Zhang (1994).

Several other deep-water fields producing offshore Louisiana are composed of thin-bedded deposits. Shew et al. (1995) worked on Tahoe and Ram/Powell prospects and incorporated data from many outcrops. According to him the key issue is to determine the internal architecture especially to evaluate bed continuity. It can be better than expected in overbank portions, covering several hundred of acres but flow transmission between channel and levees is not necessarily good.

Weimer et al. (2000) pointed out that these reservoirs are generally more complex than expected with production history of mature fields considerably different than what was predicted. They also underlined the need of integrated approach thorough the reservoir life.

CHAPTER III

METHODS

The construction of a geologically consistent reservoir model has four major steps, (1) the creation of a structural framework, (2) the delineation of the reservoir, (3) the use of seismic attributes to characterize reservoir properties and finally (4) the integration of different types of information through geostatistics for modeling of the reservoir lithofacies. The seismic interpretation was performed using Geoframe IESX package. Geostatistical study used ISATIS software.

STRUCTURAL MAPPING

Structural interpretation of the 3D time migrated survey involved salt and fault recognition. Salt is characterized by strong reflection at the top and by incoherent internal pattern. Faults were identified on sections by breaks in reflector continuity, change in phase and abrupt change in reflector dip. Time slices were very useful in the early time of mapping to help delineation of major faults. Figure 9 presents a seismic section and its interpretation, showing salt body and a major fault.

RESERVOIR DELINEATION

In order to determine the shape of the 8 sand reservoir, precise mapping of this interval was required; the method recommended by A.R. Brown in the 5th ed. of *Interpretation of three-dimensional seismic data* (Brown 1999) was followed. The main steps are:

- horizon identification at wells
- recognition of major faults

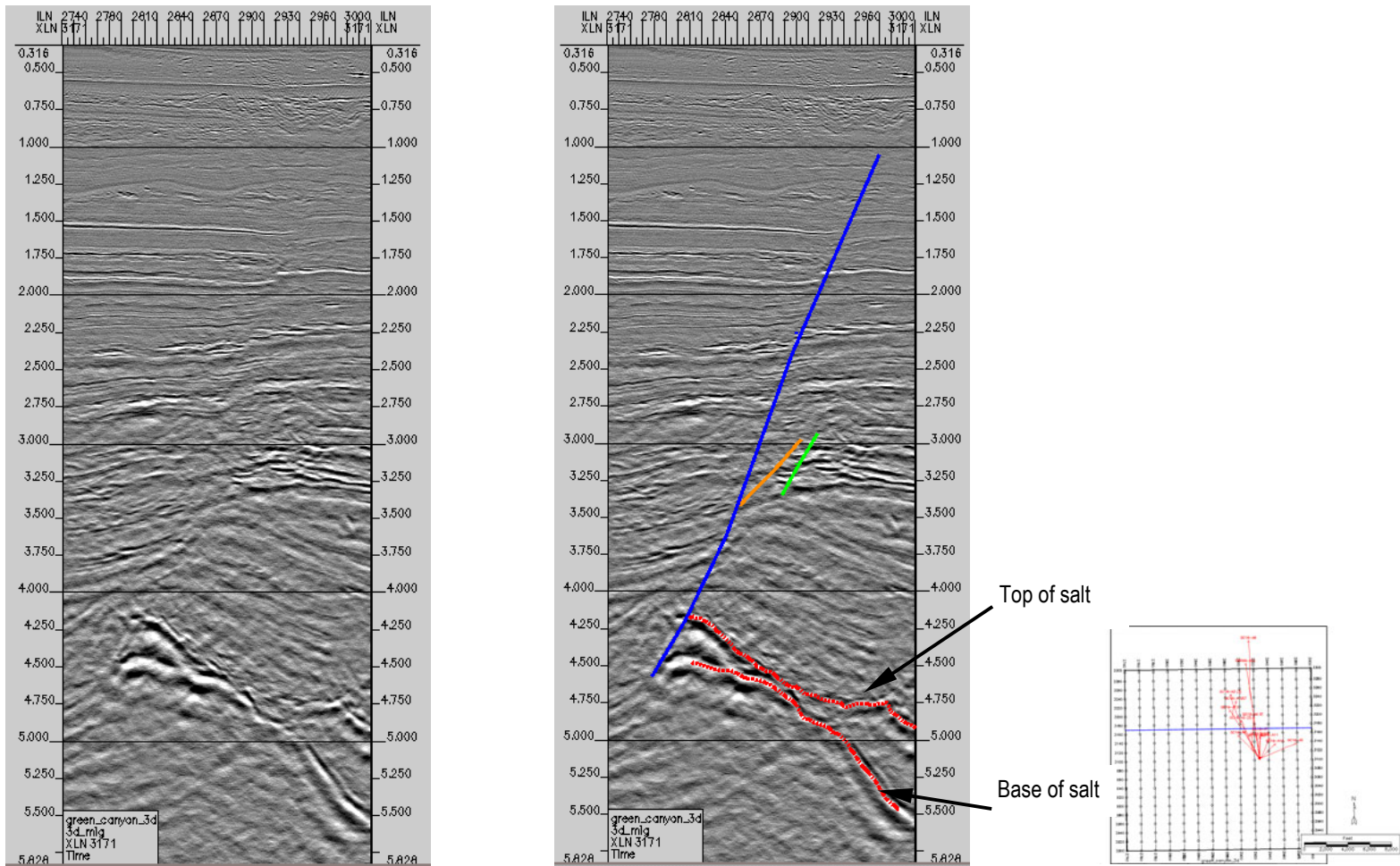


Figure 9. Raw and interpreted crossline 3170 shows high amplitude reflection associated to salt limits and a major fault.

- initial fault control
- initial horizon control
- automatic spatial tracking
- revision of horizons and faults
- time structure maps
- isochron map
- time to depth conversion

Well and seismic tying

Well paths were projected in the seismic interpretation using deviation data. Most of the wells are highly deviated. Further calibration of wells and seismic involved conversion of the depth units of well to time units using the time-depth curve derived from the check-shot surveys. The information of all the check-shots was quite consistent, as shown by Figure 10.

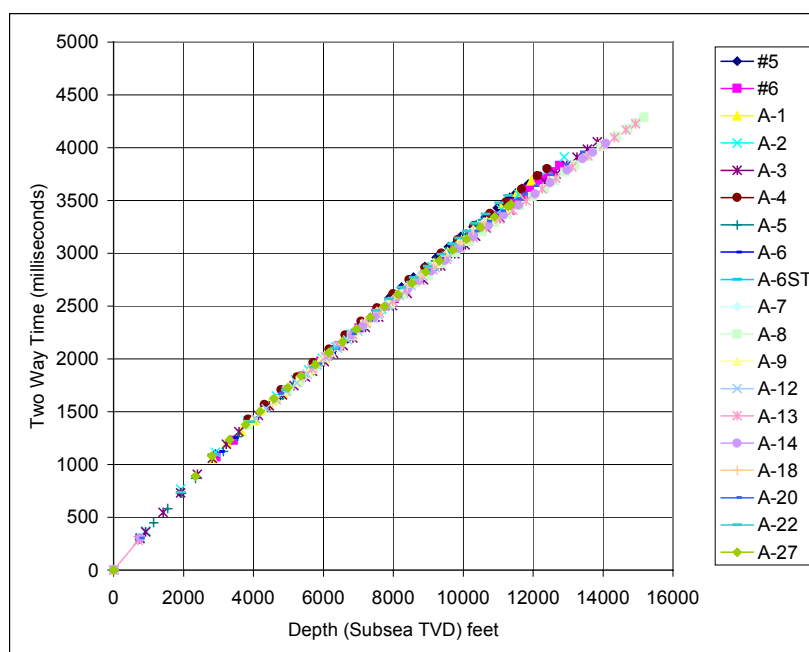


Figure 10. Check-shot data in GC 18.

The well log interpretation was performed by another graduate student (see Plantevin, 2002). The 8 sand was identified in 14 wells, top and base of sand were determined generally from comparison between resistivity curves. Separation between the ILD and the microresistivity is an indicator of permeable formation (Boyer 1999) and was found more accurate than the GR and SP variations to determine the limits of the interbedded sands. Because the thickness of individual laminations is below the resolution of the tool, gamma ray and spontaneous potential tend to give average values that are difficult to interpret quantitatively. Log analysis also provided facies interpretation and estimation of net thickness.

The top of the 8 sand is correlated with a strong positive reflection, however, synthetic generation does not show a very good match, as shown by the synthetic in Figure 11. One cause may be the high deviation of the wells, although we extracted a “tube” of seismic along the borehole path the reflector remained highly tilted. Moreover the extraction of the coefficient of reflection does not use the density log but derive this information from the velocity which as been pointed out by Burns (1986) as a reason for unreliable synthetics in the Gulf of Mexico. Mapping was then carefully extended within each fault block. Horizons were manually picked every 5 in-lines and cross-lines and after quality control by quick gridding of time structure, automatic tracking was performed using IESX ASAP module. Iteration of automatic tracking and manual control of faults and horizon is a key step for delineation of subtle faulting. For this task, we used a coherence cube and geometrical attributes based on the autotrack interpolation of the picking. Dip and azimuth were extracted. Their interest is to enhance structural features (Taner 1979): dip gives a confirmation of fault delineation and azimuth reveals discontinuities in the sand body.

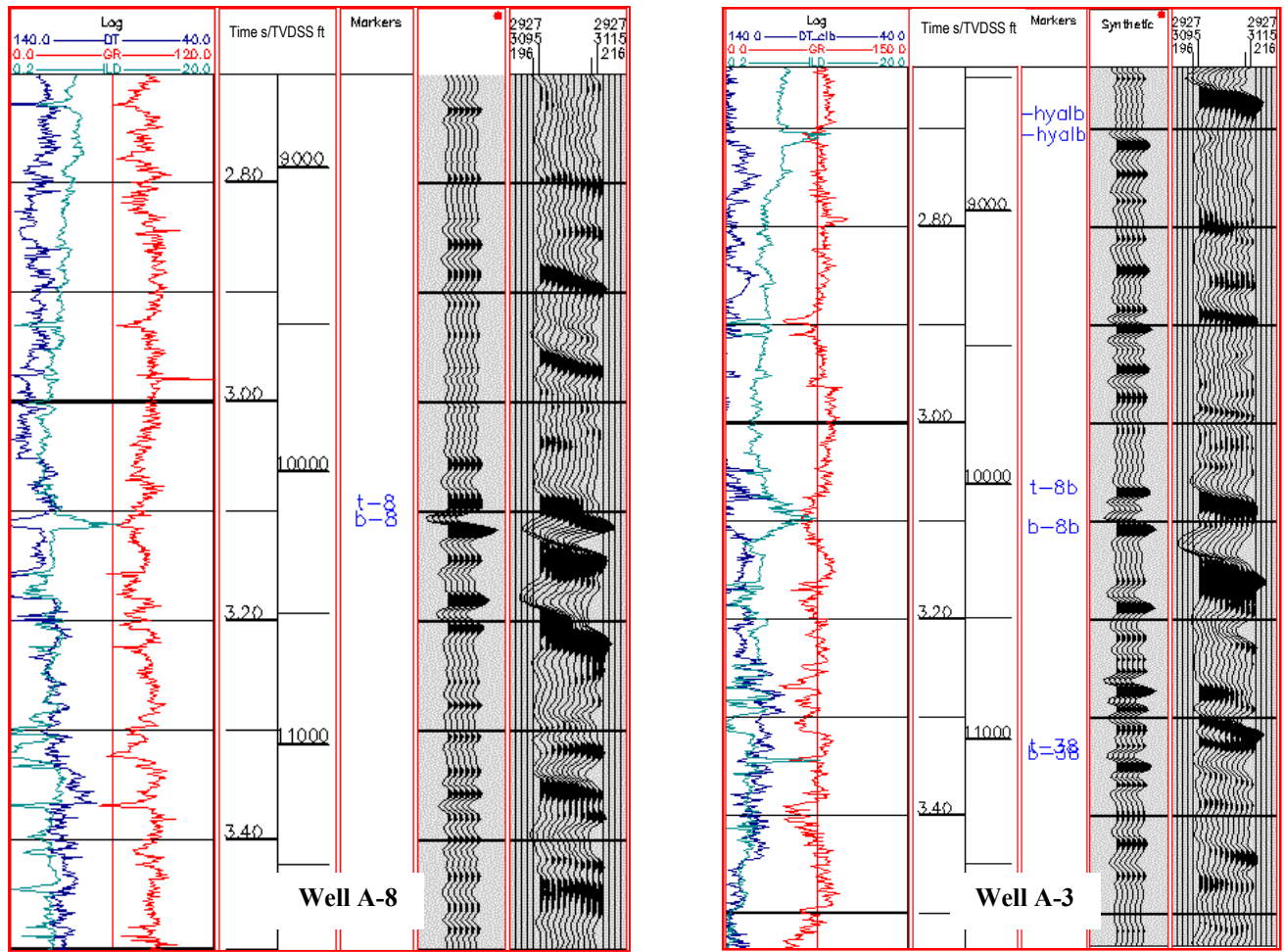


Figure 11. Composite display of well log curves, synthetic and seismic showing correlation of top 8 sand from well to seismic.

Thickness

Seismic resolution was assessed based on usable frequency at this depth and interval velocity. The Rayleigh limit gives the value of the tuning limit: maximum constructive interference between the top and bottom of the bed takes place for this value of bed thickness of 1/4 of the seismic wavelength (or, two-way time thickness is 1/2 of the seismic period). Based on the check shots the average velocity at the depth of the reservoir is 7800 ft/s, the maximum usable frequency of the seismic is 35Hz. Hence the limit is 14 ms twt or 56 ft. From the wells, the sand thickness is between 144 ft and 25 ft but because of the lack of continuity of the reflection in this interval and the low apparent frequency in this interval it is difficult to map the base of the reservoir. The base of the reservoir was picked from the wells and interpolated. Geostatistics methods discussed in the next section improved our estimation from thickness at well using the seismic isochron as a trend.

Time to depth conversion

Various methods are available for converting a horizon in time to depth, using different velocity information: generally interval velocities from seismic or time-depth curve from velocity surveys. As depth is well correlated to seismic two-way-time, geostatistical estimation techniques are an alternative way to perform this conversion (Brown, 1999; Bleines et al., 2001). Different geostatistical methods are discussed in the following section. They all honor values at each well location and seismic information can be incorporated as a secondary information. The main advantage is that it enables to derive the variance of estimation, which is an estimate of the reliability.

SEISMIC ATTRIBUTES

Attribute extraction

Seismic attributes are useful to detect subtle structural properties, geological change and variations in reservoir properties. Attribute extraction was performed using an IESX module called windowed trace (CSA) attributes.

Change in reservoir properties can be detected by reflective and transmissive attributes. Reflective attributes are computed at the level of the horizon whereas transmissive attributes involve integration over a time window. The interval of computation was of 40 ms below the top of the reservoir delineated by picking, corresponding to the maximum thickness of the reservoir.

We extracted six attributes:

- Instantaneous real amplitude: the default expression of the seismic traces extracted at the horizon.
- Maximum amplitude : the largest positive value (peak) in the window
- Minimum amplitude : the largest negative value (through) in the window
- RMS amplitude : square root of the sum of square amplitude within the window
- Arc length: total length of the seismic trace over the time window.
- Energy half time: time required for the energy within a window to attain one-half of the total energy within the entire window.

Amplitude attributes and RMS are generally good indicators of change in lithology or hydrocarbons (Chen and Sidney, 1997). Arc length indicates reflection heterogeneity and may be used to quantify lateral changes in reflection patterns. It has been used to map depositional facies in the Gulf of Mexico. Energy half time has been used to map vertical distribution of sand within the reservoir interval (Brown, 1999).

Attribute interpretation

Some attributes, such as amplitude (see Figure 12) improve the visualization of the reservoir; they provide a better display of subtle geological features.

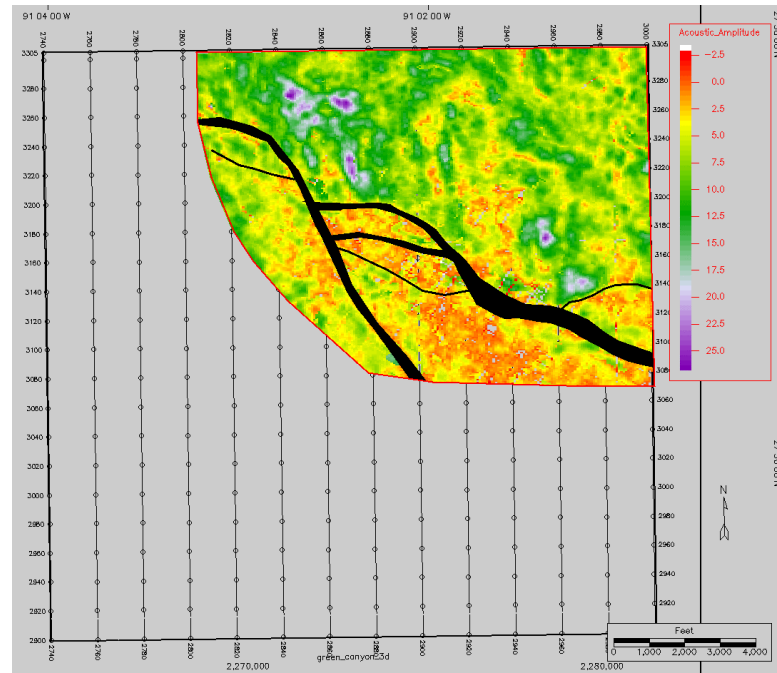


Figure 12. Amplitude map of the top of the reservoir showing low amplitudes (red) in the southwest part related to variable quality of the reflector and elongated low amplitude trend in the northwest interpreted as discontinuities in the reservoir.

In order to extract quantitative information from the seismic, we attempted to correlate these attributes with well data. The values of the attributes at well locations were extracted using a program in Visual Basic because IESX only allows to extract the value at the closest trace, which can be pretty inaccurate. The well can be mispositioned due to uncertainty of deviation data and seismic migration. Especially in this data set where most of the wells are highly deviated, and many located very close to faults. With this program we were able to check the consistency of the extracted values. Then we computed the average of the 5 closest traces corresponding to a 130*82 ft bin.

Average values of porosity and net thickness were estimated at 11 well locations (see Plantevin, 2002). In these interbedded reservoirs the average value of porosity has little significance as it represents the average of shale and sands. The correlation coefficients were computed between attributes and porosity and net thickness evaluated at well. Results are displayed in Table 1. The correlation between average properties at wells and

Table 1. Correlation coefficients between seismic attributes and well properties. The correlation is generally non significant except for net thickness, gross thickness and energy half time (abbreviated e-half).

	net thick ft	gross thick ft	poro.	e-half	amp- max	amp- min	arclen	dom freq	rms
net thick ft	1.00	0.99	0.37	0.79	-0.18	-0.02	-0.15	0.50	0.20
gross thick ft	0.99	1.00	0.39	0.70	0.19	0.16	-0.21	0.52	0.22
porosity	0.37	0.39	1.00	0.19	0.24	0.10	-0.11	0.20	0.18
e-half	0.79	0.70	0.19	1.00	0.06	-0.19	0.14	0.48	0.42
amp-max	-0.18	0.19	0.24	0.06	1.00	0.17	0.03	-0.12	0.49
amp-min	-0.02	0.16	0.10	-0.19	0.17	1.00	-0.97	0.19	-0.63
arcleng	-0.15	-0.21	-0.11	0.14	0.03	-0.97	1.00	-0.26	0.68
dom freq	0.50	0.52	0.20	0.48	-0.12	0.19	-0.26	1.00	-0.02
rms	0.20	0.22	0.18	0.42	0.49	-0.63	0.68	-0.02	1.00

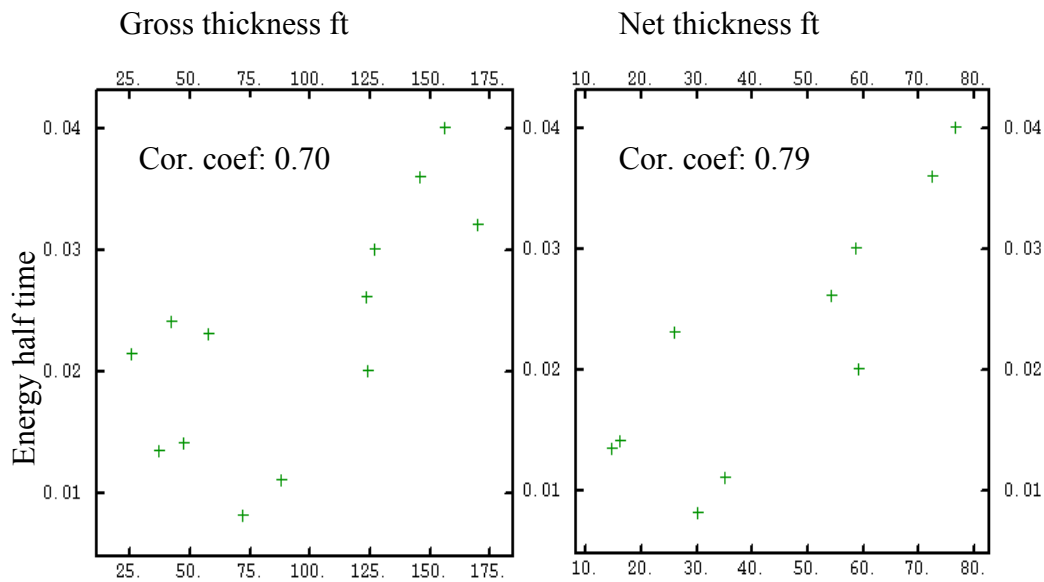


Figure 13. Scatter plots of seismic attribute (energy half time) versus gross and net thickness measured at wells.

seismic attributes is generally poor except for half energy and net thickness. We also find a very good correlation between net and gross thickness. The lack of correlation between porosity and attributes Yet, because of the small number of wells, the interval of confidence of the correlation is poor. For a correlation coefficient of 0.79, such as between half energy and net thickness the interval of confidence at 95% and for 11 samples is 0.38-0.94. The correlation coefficient is an indication of linear correlation and is very sensitive to outlying values (Schultz et al. 1994, Kalkomey, 1997). Hence it is important to check the consistency of the correlation directly on scatter plots (Figure 13).

DATA INTEGRATION USING GEOSTATISTICS

Introduction

Modeling of the 8 sand reservoir followed a two-step approach: 1) the determination of the reservoir shape and average reservoir properties, 2) then determination of small-scale variability. Several authors recommend this methodology when dealing with reservoirs that combine complex architecture and small-scale heterogeneities (Alabert and Massonnat, 1990; Weber and van Geuns, 1990; Johann et al. 1996; Beucher et al. 1999, Jordan et al. 1995). Internal heterogeneities can be studied from core and log data. However well data do not give any information on their lateral extension especially in this channel/levees environment, as correlation of individual thin beds is virtually impossible. The lateral variability of the reservoir must be inferred from the seismic information. The final objective is to reconcile these two types of information.

Seismic provides the geometry of the reservoir and some stratigraphic limits. Seismic attributes also show relationships with reservoir properties. Because of its dense coverage it is interesting to extract geological information from seismic, this can be done following different approaches (Beucher et al., 1999; Johann et al., 1996):

- seismic facies analysis based on seismic pattern recognition,
- calibration of seismic attributes to predict facies proportion.

With our data set, pattern recognition of the 8 sand was not possible, as the stratigraphic features (such as channel) are too subtle to be directly mapped. However variations in thickness and net pay could be studied from seismic data. Based on this information the overall shape of the reservoir and the direction of the main flowpath could be determined. In a second step, we focused on the representation of small-scale heterogeneities. Stochastic simulations of lithofacies have proven effective techniques to account for the incomplete information at fine-scale while preserving the internal variability (Srivastava 1994). Simulations enable the construction of multiple, equiprobable realisations of the reservoir that honor two types of statistical constraints: the lateral continuity and the frequency of each facies.

Estimation of thickness

The first step was to get the gross thickness of the reservoir. Many different geostatistical techniques are available to integrate well and seismic data. The selection depends particularly on the quality of the correlation between the two types of data. Table 2 presents a comparison of common methods (Isaaks and Srivastava, 1989; Hohn, 1999; Doyen, 1989; Xu et al., 1992). In our case, the information of the seismic interpretation was exploited using the collocated cokriging approach with Markov hypothesis (Xu et al., 1992; Doyen et al., 1996). This method uses the seismic isochron as a background variable to estimate the thickness. Its main advantage is that it avoids deriving the spatial model from poorly distributed data such as well information when we can rely on a dense and reliable background variable such as seismic. It takes full advantage of the seismic information: the cross-variance (C_{ws}) is derived from the covariance (C_s) of the background variable (here the seismic), simply scaling it by the ratio of the covariance and the correlation between the two variables:

$$C_{ws}(h) = \left(\rho_{ws} \sqrt{\frac{C_w(0)}{C_s(0)}} \right) * C_s(h)$$

This estimation technique honors the values at well locations and incorporates a trend that varies locally.

Table 2. Comparison of geostatistical estimation techniques. From Isaaks and Srivastava (1989), Hohn (1999), Doyen et al. (1996), Xu et al. (1992).

Method	Description	Data required	Pros	Cons
Ordinary kriging	Kriging is a weight averaging method similar to inverse weight distance but kriging weights depend on a model of spatial correlation.	Stationary variogram.	Best linear (minimum variance) unbiased estimator. Variance of estimation.	Accurate only with regularly sampled data. Smooth estimation. Stationarity required.
Kriging with external drift	Superimpose to the simple kriging estimation a local drift represented by a linear regression on the secondary data.	Variogram (of hard data) Computation of a polynomial drift based on the average plane fitted through the data points.	Fast: the kriging system is small. Accounts for non stationarity	Dependent on the quality of the correlation between the two variables. The estimation error does not take into account the variability of the drift variable
Cokriging	Kriging of different types of data at the same time.	Variograms and crossvariogram should have the same range and be a linear combination of elements that ensure positive definiteness	Integrated different types of data.	Smooth, secondary data integrated in a global structural model. Not possible with dense secondary data the kriging matrix becomes singular.
Collocated cokriging	Includes the seismic value at each point. Retains the secondary data closest to the location where the primary data is modeled	Same as for cokriging	The link between the two variables is local.	Cross-covariance still needs to be modeled.
with Markov hypothesis	All variograms and cross variograms are proportional for all distances	Variogram of hard data and cross-variance derived by scaling the structural model computed from the seismic, using the experimental values of the ratio of variance of the two data sets and the coefficient of correlation	Avoids modeling cross variance	The secondary variable needs to be informed at all nodes where estimation is computed.
Indicator kriging		Selection of cutoffs Indicator variogram models	Enhances connectivity patterns useful maps for decision making	

Comparing the two variograms in Figure 14 shows the advantage of using Markov collocation. In this specific case the range could not be inferred with confidence from the wells' information because sparse well data are not homogeneously distributed. The variogram extracted from the seismic is much more precisely defined.

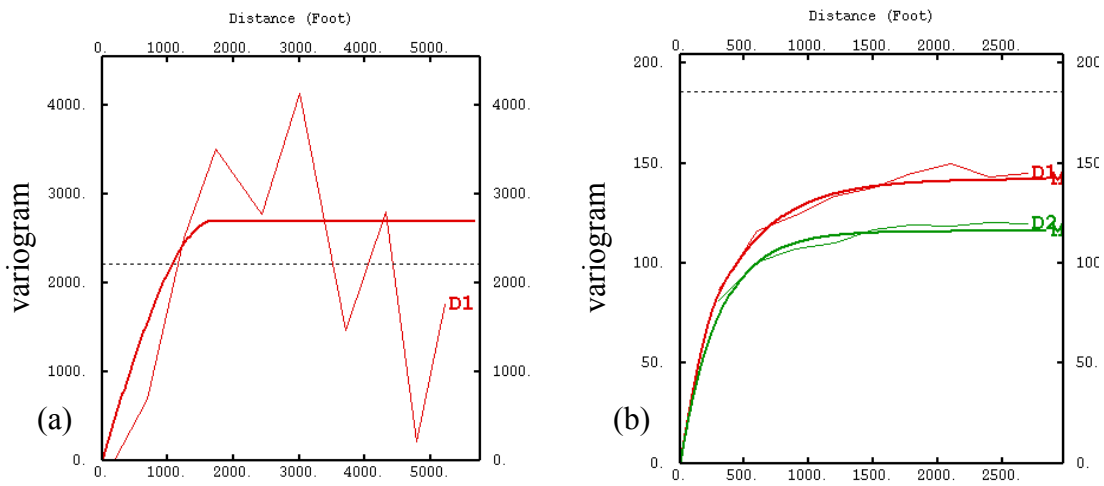


Figure 14. (a) Omnidirectional variograms of the gross thickness from well information only. (b) Variogram of reservoir isochron derived from seismic, D1 is the X axis, D2 the Y axis. Thin lines are experimental variograms, bold lines are models. The dotted line indicates the variance of the data.

Net thickness estimation

Net-to-gross is very difficult to measure from logs in these laminated reservoirs: gamma ray log commonly used for this estimation does not have here the resolution required (Hansen and Fett, 2000). In our case, net thickness was estimated from density and neutron logs based on calibration with cores (see Plantevin, 2002). This evaluation was possible only in 11 wells. The good correlation between net thickness and gross thickness is interesting but it does not give any additional information. Conversely, the correlation with a seismic attribute (energy half time) provides an alternative approach to evaluate the lateral variations of reservoir quality.

Incorporating the seismic attribute as a secondary variable, we can estimate the net thickness. We used the collocated cokriging approach (Xu et al., 1992; Doyen, 1989) with a classical model of cross variogram that gives a close agreement with the attribute map.

Heterogeneity representation

The core issue in building a reservoir model is the internal variability. In thin-bedded turbidite reservoirs, heterogeneity is generally controlled by the distribution of the most porous facies: channels and proximal levees interbedded with more shaly deposits (Alabert and Massonnat 1990, Handyside et al, 1992). Study of core data of the 8 sand (see Plantevin 2002) also led to the definition of three facies with distinctive sand/shale ratio.

The choice of the simulation technique to reproduce this variability has a enormous impact. To model litho-facies, that is to say non continuous variables, the most common methods are boolean or object based techniques and different types of sequential simulation (Srivastava 1994, Galli and Beucher 1997, Haldorsen and Damsleth, 1992; Haas and Dubrule 1999). Boolean methods consider facies as objects defined by their shape that are simulated over a background, for example sinuous channels in an alluvial plain (Shmaryan and Deutsch 1999). Characteristics of the object include size, orientation and anisotropy. Sequential simulation techniques follow a completely different procedure. After a random path is defined to visited each grid node, a conditional probability distribution is estimated (depending on the data already simulated) at the current node and a random value is extracted from this probability distribution. This value is included in the dataset and the process is repeated until all nodes are simulated. These methods differ by the way the probability distribution is built. In the sequential indicator approach, the shape of the distribution does not assume a classical function but is computed from the data giving a series of thresholds (Journel and Alabert, 1990; Suro-Perez et al., 1991; Caers et al., 2000). The method used for this

study is a truncated Gaussian approach (Matheron et al., 1987, Ravenne and Beucher 1988).

At each location the facies is described using an indicator function, $Z(x)$, based on a gaussian probability distribution, $Y(x)$:

$$Z(x) = \sum I_{a_{i-1} < Y(x) < a_i}$$

The point x belongs to facies (i) if $a_{i-1} < Y(x) < a_i$.

In ISATIS software, $Y(x)$ is simulated sequentially honoring the range of the prevalent facies (Bleines et al. 2001). The thresholds a_i are directly related to the proportion of each facies and are ordered. In our case, the facies are characterized by a variable sand fraction. The simulation is directly conditioned, as the proportions of each lithofacies are determined at each horizontal level via vertical proportion curves (see Figure 15, from Doligez et al., 1999). Vertical proportion curves correspond to the percentage of facies computed in the well at different levels parallel to a reference (Eschard et al., 1998). Lateral variations in the proportions of each facies also have to be taken into account. Seismic derived map of thickness and net pay enabled us to distinguish lateral zones in the 8 sand, each characterized by its sand proportions.

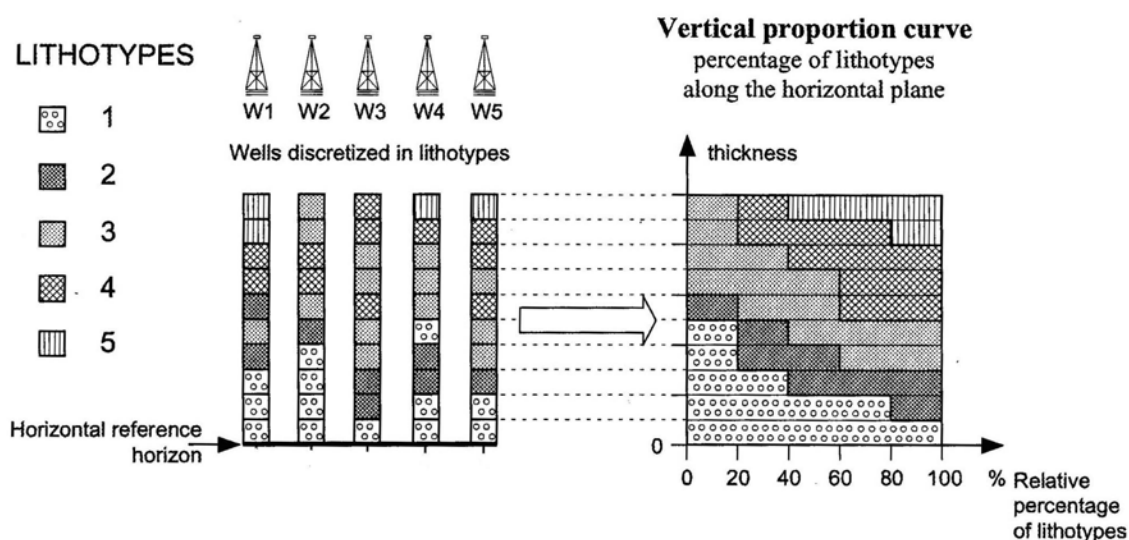


Figure 15. Principle of computation of proportions curves. The relative proportion of facies is characterized vertically from well data. (Modified from Doligez et al., 1999).

CHAPTER IV

RESULTS

This chapter presents the results of the reservoir characterization: 1) the structural and stratigraphic framework, 2) the extraction of geological information from seismic and 3) the geostatistical modeling of lithofacies.

STRUCTURE AND STRATIGRAPHY

The major structural features of the field are the salt geometry and the fault system. The salt forms a ridge culminating in the Southeast corner of the field in a diapir that reaches the surface. The crest of the ridge, oriented NW-SE is lying between 4050 and 5050 ms. The structure map of the top of the salt in Figure 16 shows that the ridge is globally east dipping and the isochron in Figure 17 indicates that it is composed of two elements, as shown also by the cross-section.

The block is traversed by a salt detachment fault dipping down to the basin (blue on Figure 19). Several secondary listric faults intersecting the 8 sand have been mapped, they all exhibit the same pattern, NNW-SSE to NW-SE trending, SW dipping. Figure 20 shows the time structure of sand 8 with the intersection of the main faults and a cross section (Figure 19) indicates their vertical extend.

The structure at the top of the reservoir is shown in depth by Figure 21. The upthrown block is an anticline oriented north south and dipping north. The top of the 8 sand is lying between 9500ft and 10500ft. The crest of the structure is located along the fault. The strong dip of the field, opposite to the regional basin dip, seems induced by salt movements. The gradient is steeper in the eastern side and close to the diapir. The comparison of the isochron indicates that salt withdrawal was really significant after deposition of the 8 sand.

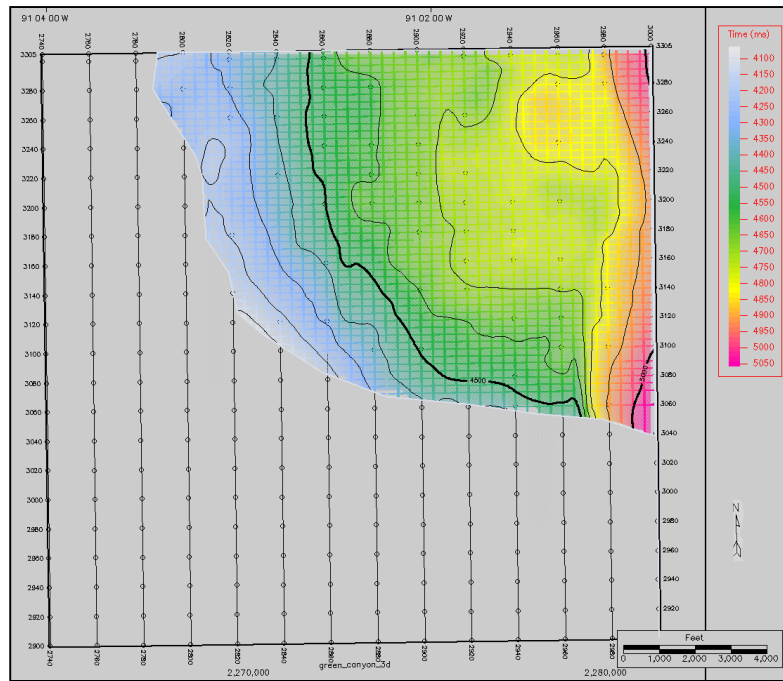


Figure 16. Structure map of the top of the salt ridge

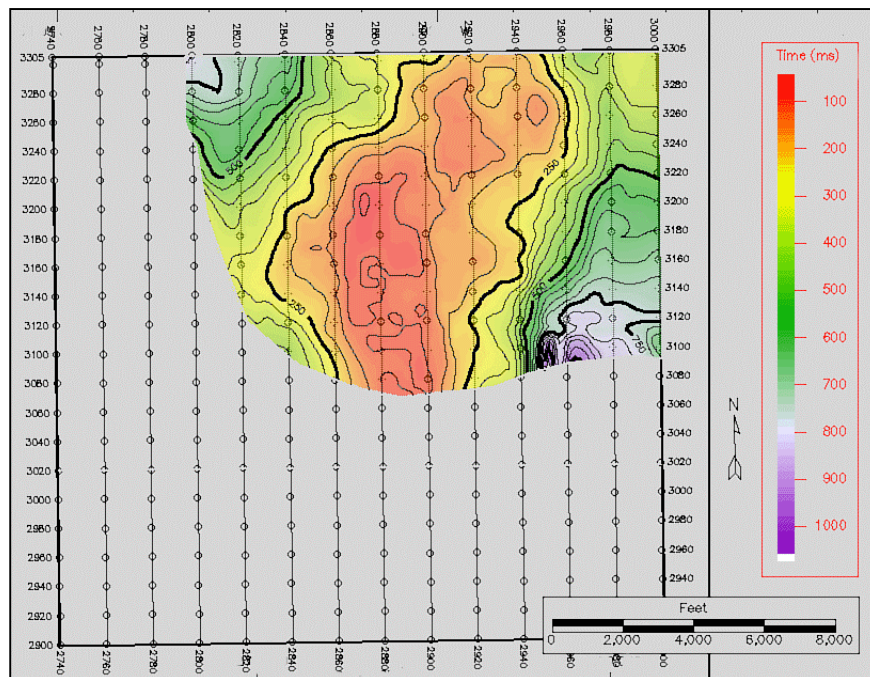


Figure 17. Salt isopach, two salt bodies separated by a thinner zone in red <100 ms

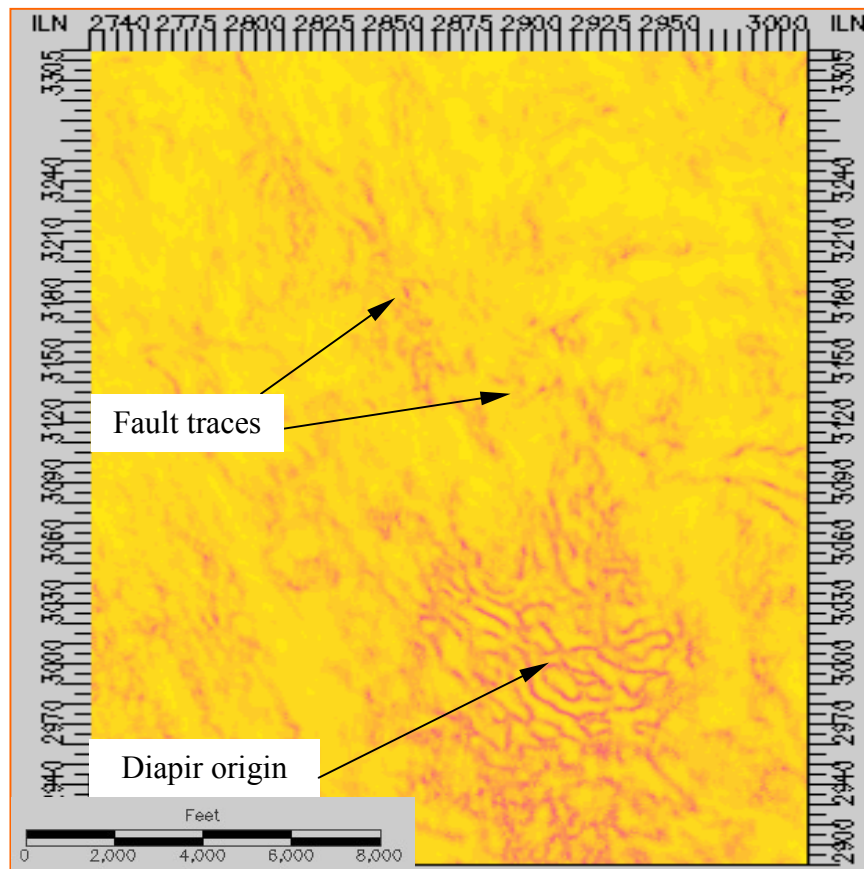


Figure 18. Coherence slice at 3176 ms (intersects the reservoir) showing some fault traces and the origin of the diapor in the southeast.

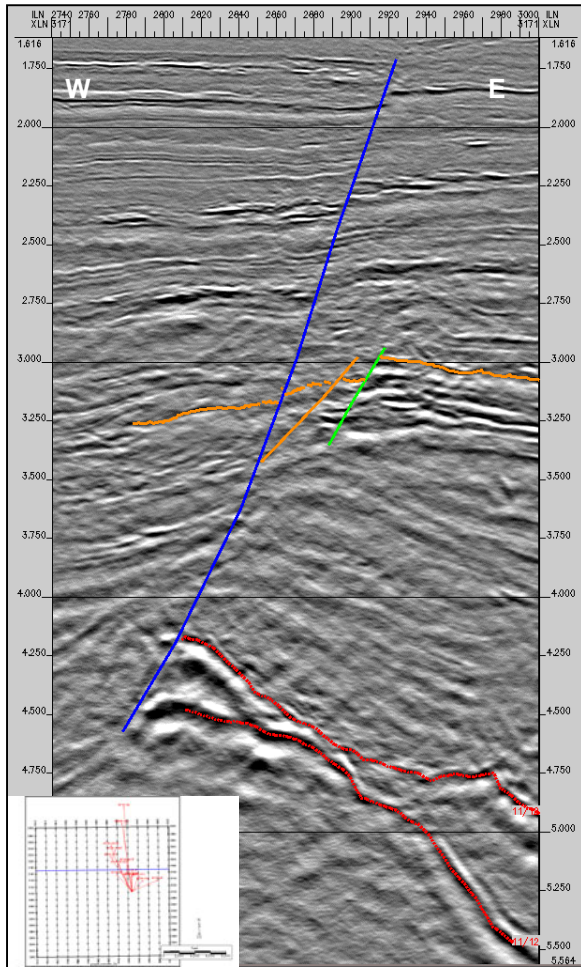


Figure 19. Interpreted section showing salt ridge and major faults intersecting the reservoir. Orange horizon is top of sand 8.

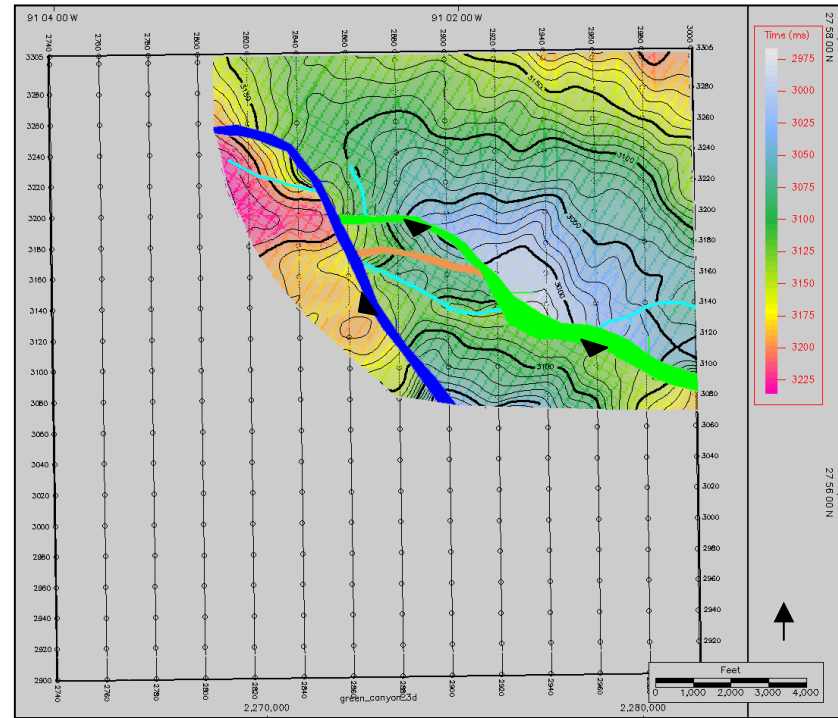


Figure 20. Time structure of the top of the 8 sand reservoir with trace of major faults.

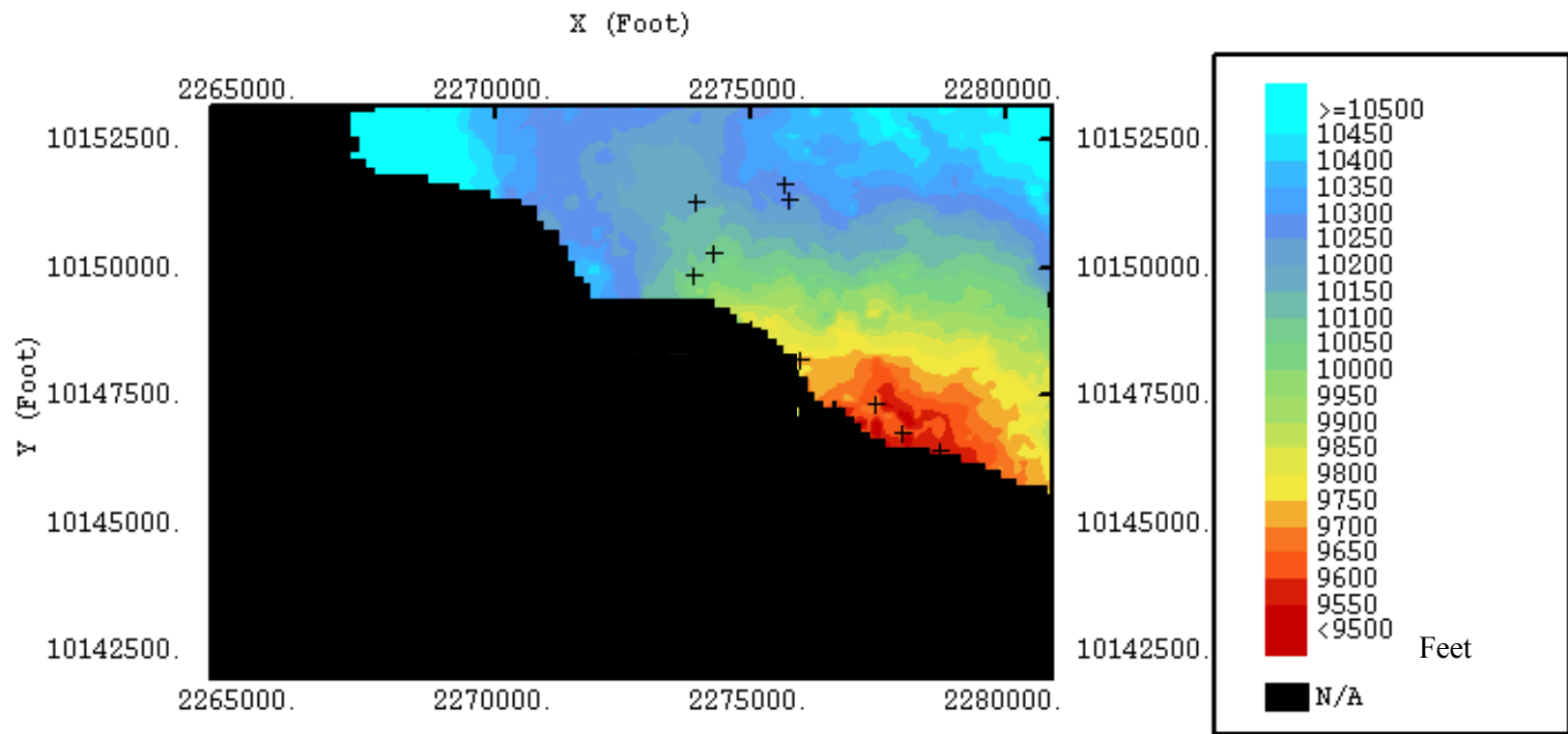


Figure 21. Depth structure of the top of the reservoir.

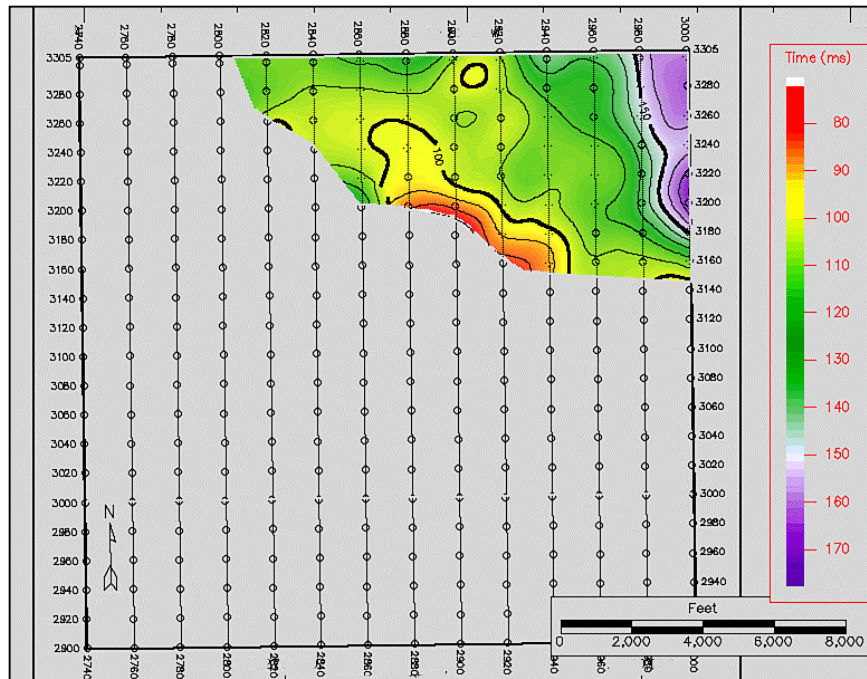


Figure 22. Seismic derived isopach between the top of the reservoir and the top of the CM sequence (1.4 Ma) indicating beginning of salt withdrawal early after deposition.

Stratigraphy

The seismic response of the 8 sand interval is characterized by shingled patterns typically representative of channel levees depositional environment. The stratigraphic features are very subtle and difficult to detect in this environment as individual channels are usually below seismic resolution. Amplitude map (see figure 12) shows elongated trend of low amplitudes that can be related to discontinuities in the reflector. Figure 23 shows a cosine of phase display of a section. The continuity of the reflector is enhanced compared to the usual amplitude display. It indicates overlapping of the eastern reflectors. This configuration suggests for the northern zone lateral stacking and possible discontinuities in the reservoir. The southern zone has a poor seismic response, and the relationship between the two units can not easily be distinguished on the seismic.

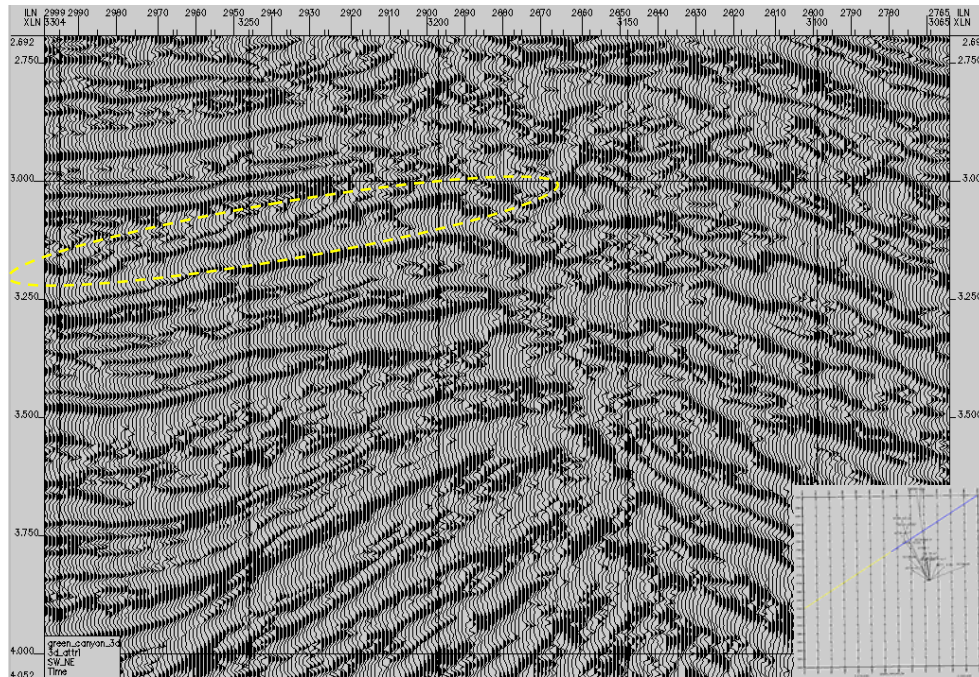
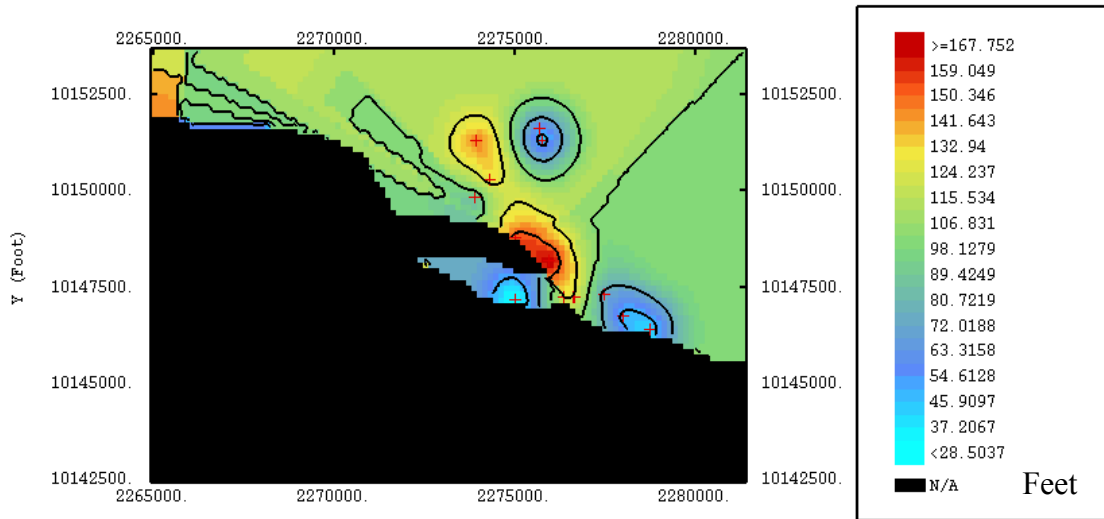


Figure 23. Cosine of phase display of a section enhancing the continuity of the reflector. It shows the shingled pattern of 8 sand and overlapping of the eastern reflectors.

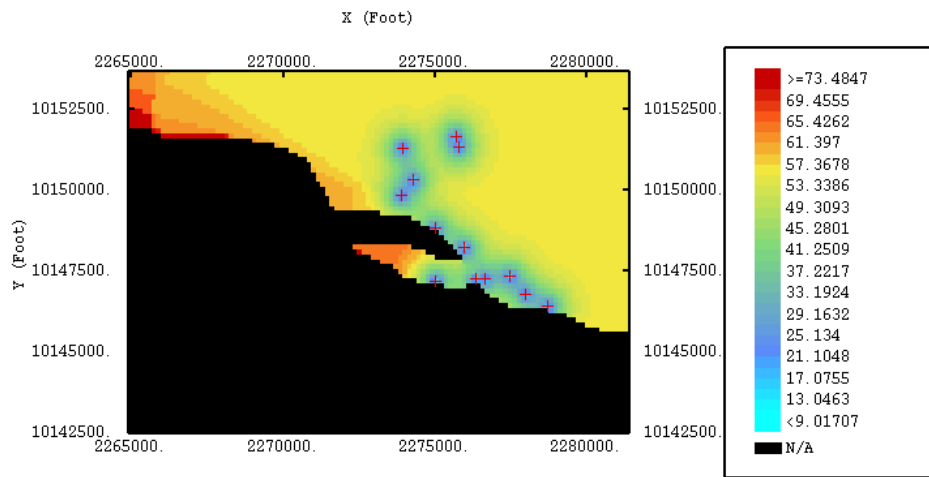
GEOLOGICAL INFORMATION FROM SEISMIC

Thickness

The generation of thickness map enabled to see the general orientation of the system. The first map was generated using well data only with the ordinary kriging method (Figure 24). It shows the “hole pattern” produced by this estimation technique when constraining data are too scarce. Although it does not shows realistic shapes it enables us to detect the low reliability zones, the corresponding estimation variance map shows the low reliability of the estimation away from the wells.



a)



b)

Variance

Figure 24. a) Thickness map derived from well data only and b) its associated variance of estimation. Away from the wells the uniform value shows the lack of information.

The second maps incorporate the seismic isochron information to infer spatial variations away from the well, see Figures 25 and 26.

Reservoir thickness varies from 170 to 70 ft. The map (Figure 26) shows an elongated thicker zone above 100 ft oriented North South and bent along the fault. This area matches approximately the crest of the structure and can be considered as the main reservoir unit. The width of this unit varies from 2500 ft in the north to 1000 ft along the fault. All the producing wells are located in the area where the thickness of the reservoir exceeds 100 ft.

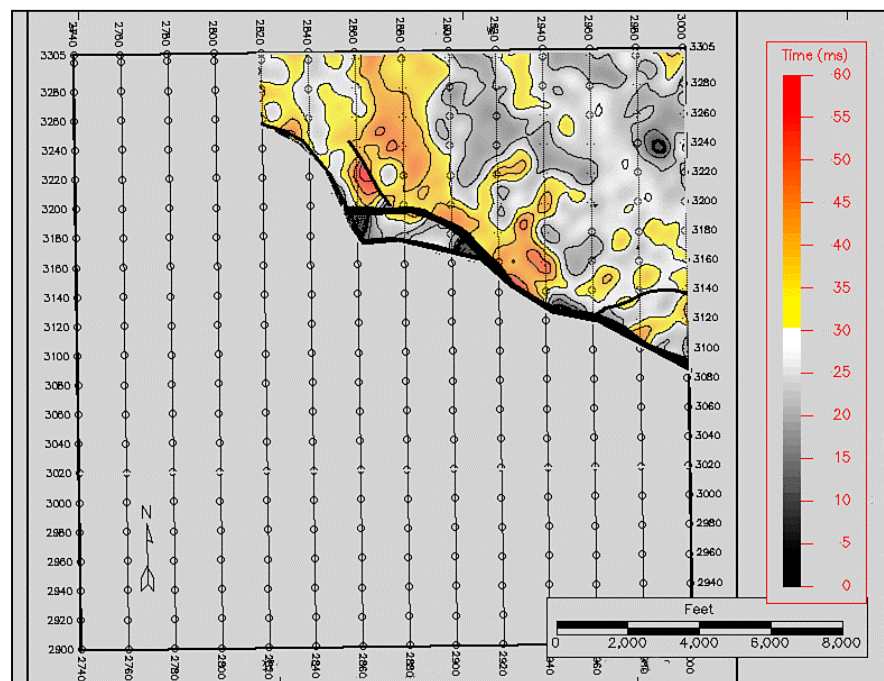
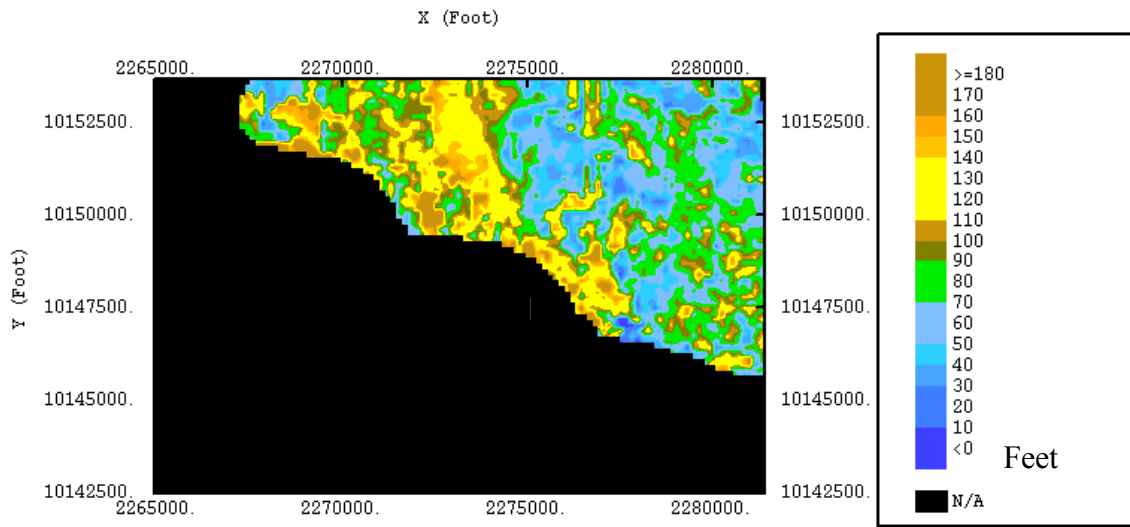
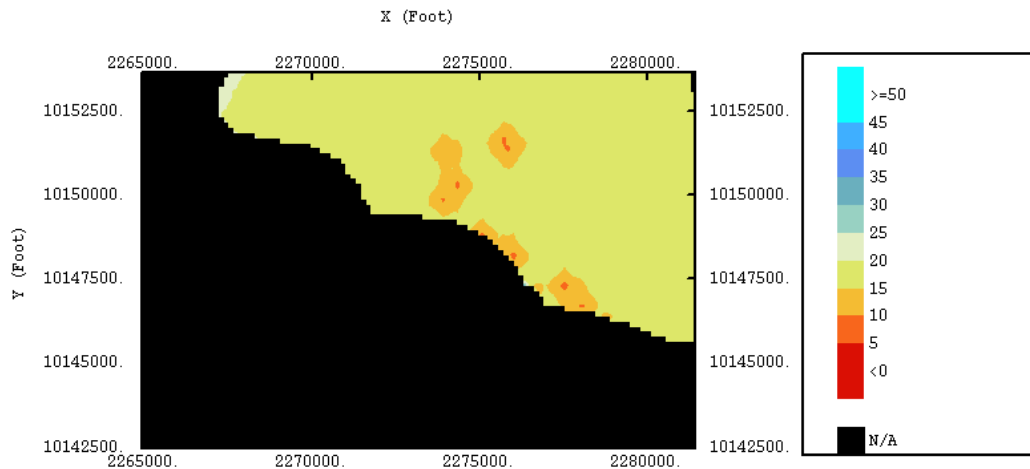


Figure 25. Seismic-derived isopach of the 8 sand reservoir.



a)



b)

Variance

Figure 26. a) Thickness map incorporating seismic and well information and b) associated variance of estimation, much reduced compared to the case with well information only Figure 24.

Net thickness estimation

Evaluating net thickness is very important in channel/levees reservoirs, this parameter significantly affects flow units as it generally correlates with vertical and lateral connectivity (Khan et al., 1996). The net thickness was estimated at 11 well locations. The good correlation of net thickness with a seismic attribute enabled to derive the map shown in Figure 29. Again we observe a north south trend, well correlated with the thickness, especially at the eastern edge of the reservoir unit.

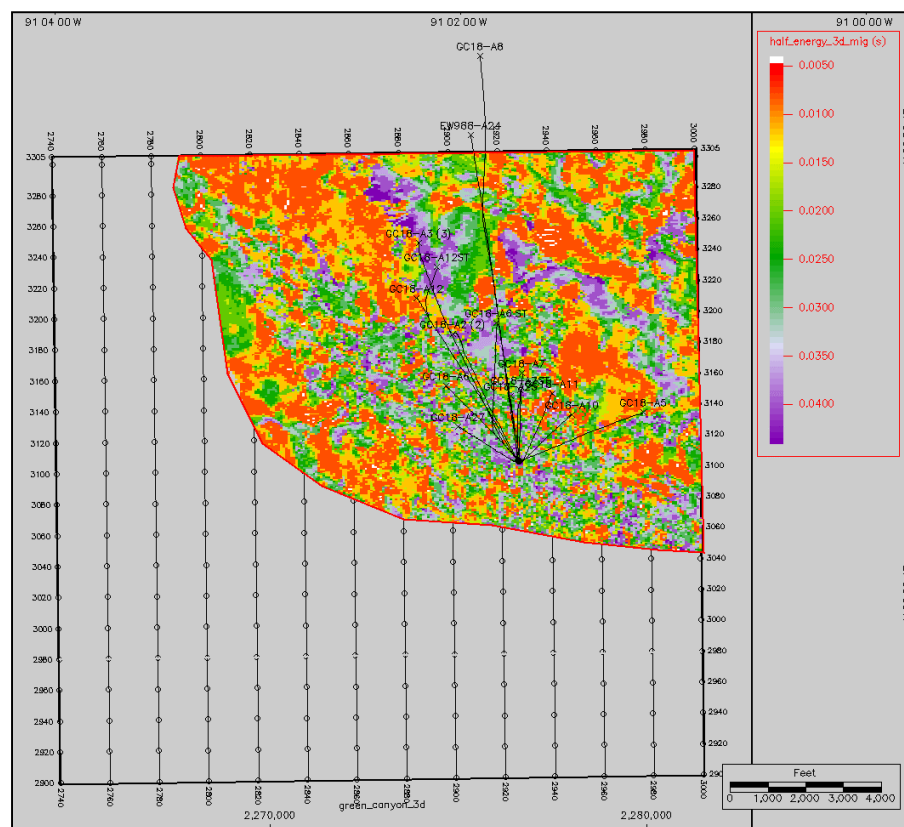


Figure 27. Map of the seismic attribute (energy half time) used to derive the drift of net thickness.

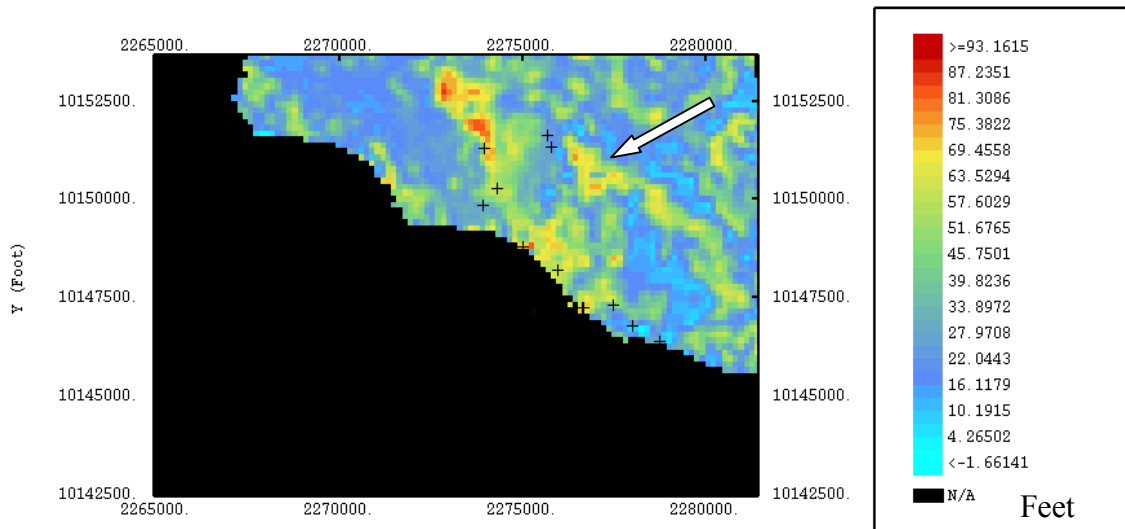


Figure 28. Net thickness map incorporating well and seismic attribute information. The arrow shows an anomaly where the net thickness is equal to the gross thickness.

The discontinuities between the northern and the southern zones can also be noticed. The good correlation with the thickness was expected in this environment; conversely the preeminent elongated zone in the eastern part is suspicious, as it lacks correlation with the thickness and has no well confirmation.

The results are consistent with our interpretation of the system; an elongated narrow zone shows the best net thickness flanked by intervals of decreasing net-to-gross. These features however are field related. They do not characterize a general channel-levee system but the result of the specific depositional arrangement in this block. The main feature is the rapid lateral variability of the properties. The variogram extracted from this map shows a range of 850 ft, which gives an indication on the lateral extension of the seismic-derived facies.

GEOSTATISTICAL MODEL

Reservoir modeling was based on vertical proportions curves of facies derived from core and log analysis and on lateral change of the average net pay reflecting the evolution from proximal to more distal regions of the channel/levee system.

Facies definition

Core description distinguished five facies. Three of them were retained to represent the reservoir heterogeneity (see Plantevin, 2002).

- Facies A is made of thick intervals of clean sands with very rare and thin shale laminations. It is thought to be a “channel” facies. The sand fraction is very high, with an average of 81%
- Facies C is made of laminated sands; the thickness of each sand bed varies between 0.2 and 5 inch and has an average of 2 inches. It is the typical levee facies. The average percentage of sand is 54%.
- Facies E is shale dominated with some thin sands beds below 1 inch thick. It can be the overbank facies, the sand content is very low: 6%.

The assumption for reservoir modeling was that heterogeneity in the reservoir is mainly controlled by the proportions of each facies as they show distinctive petrophysical properties and are not affected by diagenetic cementation (Plantevin, 2002).

Reservoir zonation

Seismic derived map of net thickness enabled to distinguish two lateral zones with different average properties. In the eastern part, the average net to gross is 39% whereas in the western part along the fault it is 45%. This distinction is an important step as one of the hypotheses of simulation is stationarity, which assumes that the statistical properties are homogeneous in the region simulated. When different zones are defined based on variation in average properties, they are simulated independently.

Moreover, as the conditioning rely not only on the average facies proportion but also on their vertical association, it is important to preserve this variability. These considerations finally led to the distinction of three zones presented in Figure 29. Zones I and II cover the thickness above 120 ft and comprise all the producers. Zone I delineates the elongated trend corresponding to the highest thickness and net pay and it delineates a probable major flowpath. Zone III corresponds to the more distal parts of the levees and the thickness is only 90 ft.

The limits of each zone were drawn from the net thickness map. These boundaries between zones synthesize the seismic and geologic information. Faults are not taken into account at this stage. However, their impact (sealing or not) would have to be considered for flow simulation.

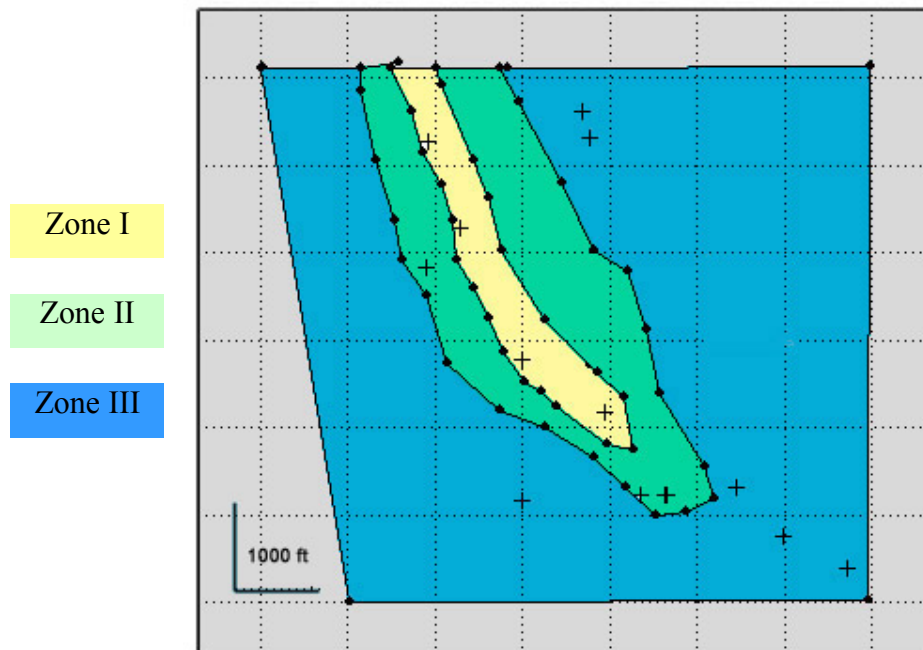


Figure 29. Zonation of the reservoir based on net thickness and facies proportion at wells. Zone I and II have an average net-to-gross of 45%. Zone I delineates the main flowpath where channel facies are more continuous. Zone I is the most distal part with an average net-to-gross of 39%. Faults are not taken into account.

Vertical Proportions

The vertical proportion curves of each zone are presented in Figure 30. The comparison of these curves shows that although zone I and II have the same NTG, the distribution of facies A is different. Zone I is characterized by a thick interval of facies A, whereas in Zone II facies A is more scattered in the upper part of the reservoir. The vertical proportion curve in Zone III shows as expected a larger proportion of the more shaly facies, facies E; and an increase of facies C at the top of the unit.

Model

The simulation was performed with smoothed curve to reduce the impact of mono-facies intervals created by the lack of samples. One realisation is displayed in Figure 34. The vertical range is based on the average length of the facies interval from well interpretation. It is of 10 ft for facies E and C and 5 ft for facies A, which indicates the thinness of the eventual channels. The lateral range was derived from the net thickness map. The underlying assumption is that because of the low total percentage of facies A, lateral variations reflect mainly the continuity of facies C, the lateral range was 850ft. The simulation was performed on a 150*150*1ft grid.

The result of the simulation are shown in Figure 30 and 31, the grid is not in structural position and shows sharp thickness variations but enable to see the vertical and lateral evolution of the lithofacies. The 3-D view (Figure 30) shows that the lateral continuity is good within each unit but the vertical continuity is variable. This is consistent with conceptual models of channel/levee systems (Shew, 1995). The simulated section (Figure 31) shows the details of facies repartition. Although these lithofacies do not represent individual beds, this realisation gives a representation of the impact of internal architecture on flow-units connectivity. Facies A, mainly composed of sand has very good permeability, facies C highly laminated has anisotropic transmissivity properties and facies E mainly composed of shale probably acts as a permeability barrier (Plantevin, 2002).

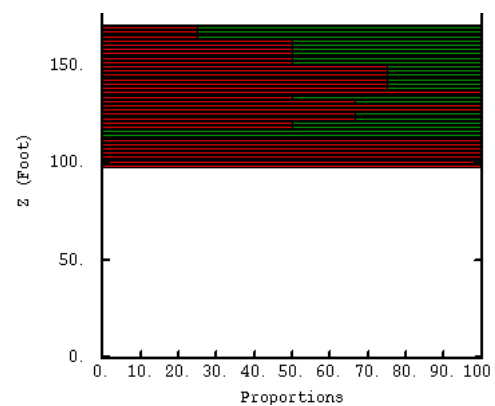
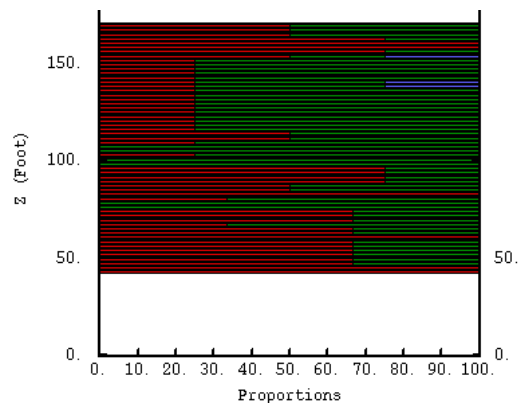
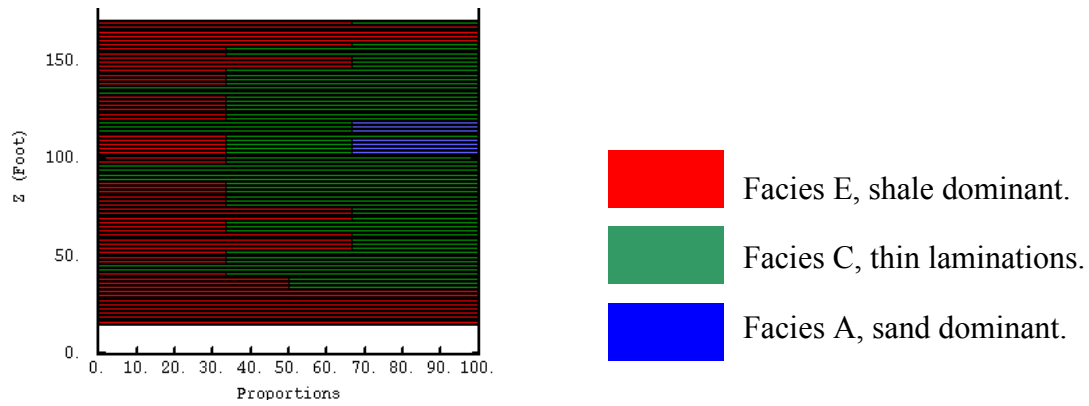


Figure 30. Vertical proportion curves generated from facies identified at wells gathered by zones to respect lateral variation in average facies proportions (Zone III with higher proportion of facies E) and vertical associations (Zone I with a continuous interval of facies A whereas they are more scattered in the upper part in zone II).

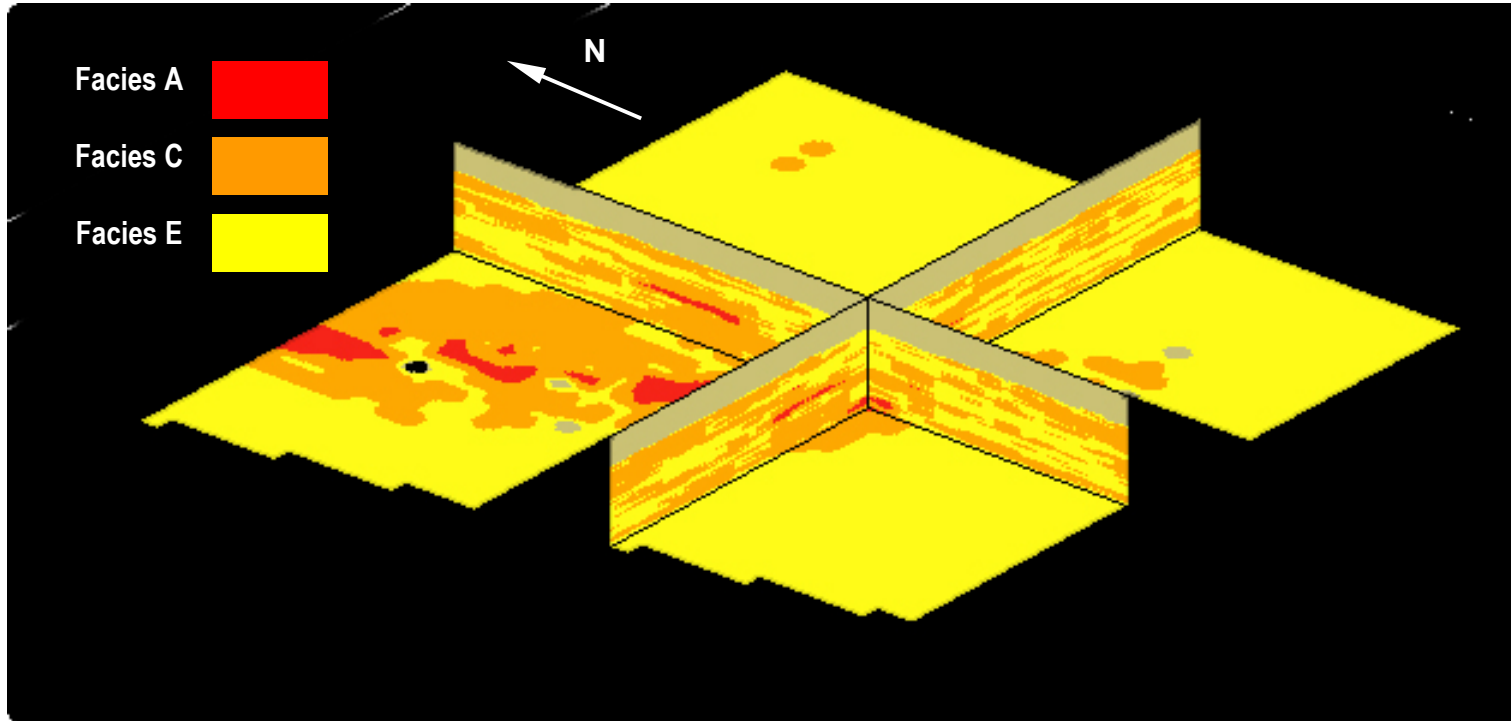


Figure 31. 3D lithofacies simulation of the 8sand on a 150*150*1ft grid with a lateral range of 850ft and a vertical range of 10 ft. Within each unit the lateral continuity is good but the vertical continuity varies.

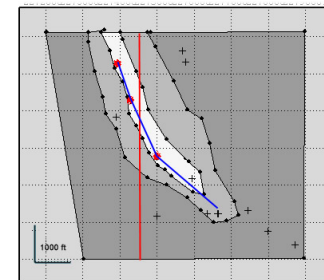
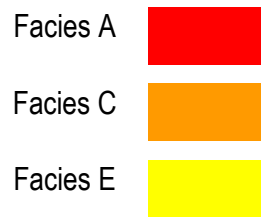
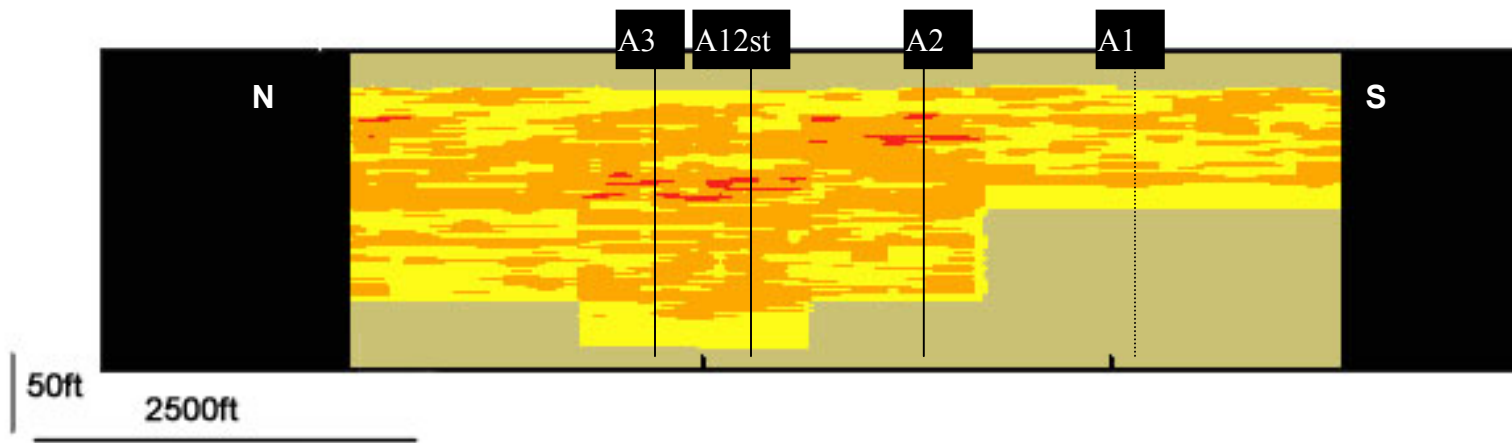


Figure 32. N-S section of the 8 sand lithofacies simulation. The separation in zones enables to represent the lateral variations in average net-to-gross. The location map shows in red the simulated section and in blue the well section of Figure 33. Vertical lines represent the projection of well locations.

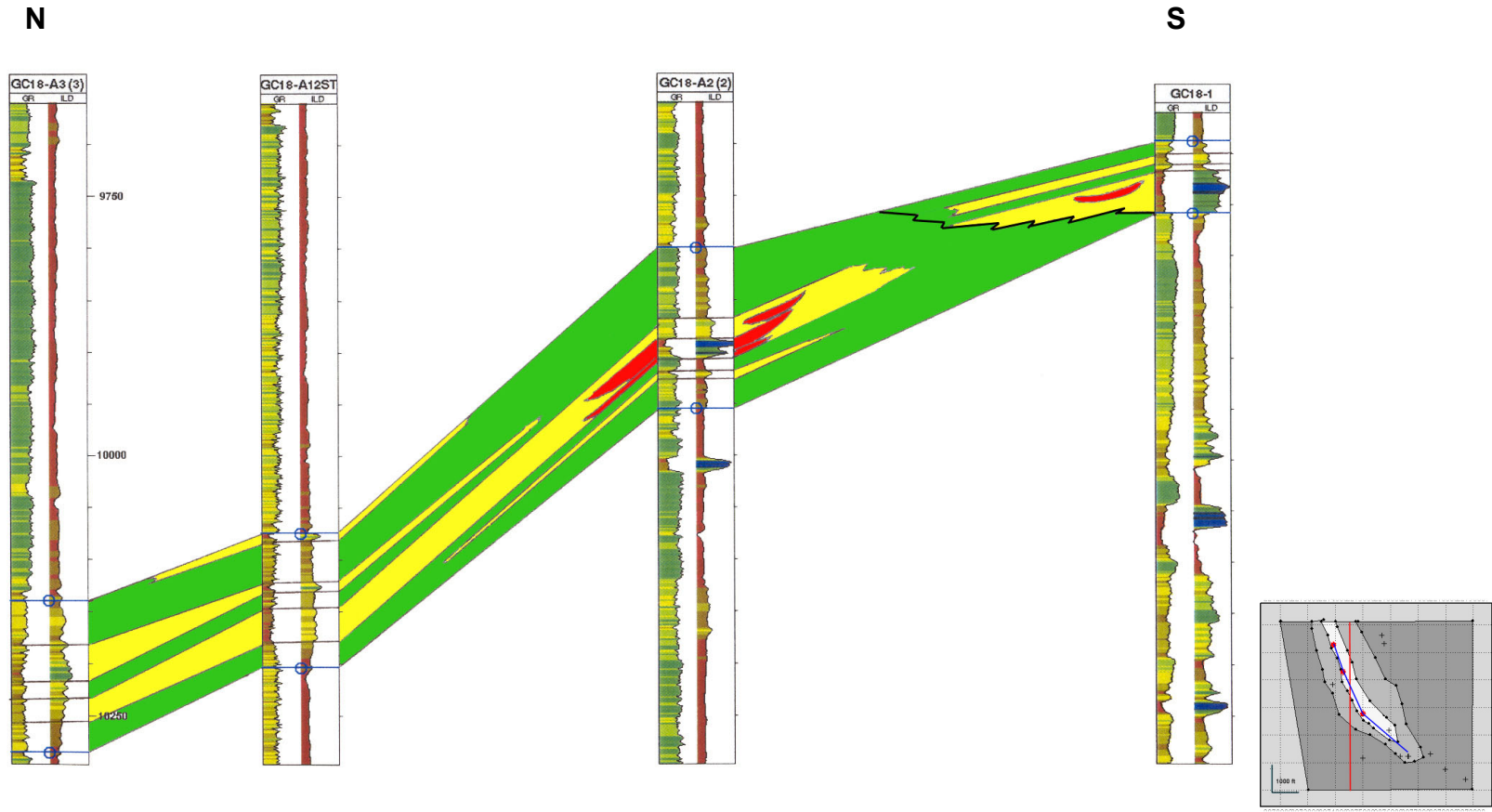


Figure 33. Well correlation of the 8 sand from Plantevin 2002. The location map shows in blue the well section and in red the simulated section of Figure 32.

The simulated section (Figure 31) can be compared with well correlation from Plantevin (2002), in Figure 32. Comparison with log correlation by Plantevin (2002) shows the consistency of the simulation with the conceptual model and the advantage to reproduce fine-scale variability to show more realistic internal connectivity patterns.

Thanks to the zonation of the reservoir based on seismic interpretation, the simulated section reflects both the regional trends and the fine-scale repartition of lithofacies.

CHAPTER V

DISCUSSION AND SUMMARY

RESERVOIR STRUCTURE

The structure of the field, with a major salt detachment fault is representative of the Outer Continental Shelf: salt mobilization creates a ridge, uplift of the ridge deforms overlying layer and initiate growth faulting (Bradshaw and Watkins, 1996).

The depositional model of the block is interpreted as a tilted turbidite system due to salt diapirism. The sediments were probably trapped on the northern side of the salt ridge. When the northern part continued to subside due to sediment loading and withdrawal the sands were tilted and formed traps. The reservoir of interest is located upthrown side of the main faults, which is fairly uncommon as the accommodation allowed by growth faulting often lead to concentration of sand immediately downthrown (Zhang, 1994). Only one well intersected the 8 sand level in the faulted block and it showed a very thin layer (25ft). One possible explanation is that the paleotopography was mainly affected by the uplift of the diapir in the southeastern part of the field and that the flow path was bent on the northern flank of the salt.

DEPOSITIONAL ENVIRONMENT

The 8 sand is believed to have been deposited a channel/levee system. Several channels may have been active through time but they are too small to be mapped on the seismic. Thickness and net pay maps suggest that the deposition occurred mainly along a single path and show the lateral evolution of the lithofacies assemblage from proximal to distal distributions.

The deposition was probably controlled by paleo-topography with accumulation of sand on the north flank of the diapir. This environment is characterized by vertical and lateral stacking leading to sharp variations in sand thickness and continuity. Yet the

estimation of net thickness revealed that average the reservoir quality over the thickness was highly dependent on the distance to the channel zone. The integration of seismic interpretation and well log interpretation enabled to build a model that reflects these regional trends and reproduce the internal variability.

GUIDELINES FOR RESERVOIR MODELING

The main interest of this integrated approach is to describe the reservoir heterogeneities at different scales:

- At the field scale, the reservoir is bounded by a fault probably sealing (from pressure data, Williams L.I. pers. com. 2000). Thickness, net pay map and amplitude discontinuities suggest that the reservoir is likely to be constituted of at least two units. One of the objectives of history matching is to confirm the non-communication of these two units produced in the north by well A-3 and A12 ST and in the south by A2, A25, and A27.
- At the reservoir scale, the average quality of the reservoir is globally linked to net thickness, the thickest part is believed to be the closest to the channel. However, the horizontal and lateral communication of individual sand layers is highly uncertain. The rapid vertical and lateral change observed in well and core data are likely to be major controls of the flow.
- The model generated reproduces the variability assessed from seismic and well interpretation. The limits of the zones have a great impact on lateral continuity. The position of these boundaries should be tested with flow simulation. A more sophisticated approach would be possible with HERESIM software developed by IFP (Doligez 1999, Eschard et al. 1998, Beucher et al., 1999). This software allows to build 3-D proportions matrix that account quantitatively of the lateral change in facies proportions.
- The proportion of each facies, especially A and E that shows distinctive permeability values, should be part of a sensitivity study to asses uncertainties.

- The lateral range of lithofacies within each unit can also have a major impact on connectivity and should also be tested.

SUMMARY

For an optimal exploitation of a reservoir, a geologically consistent model is required. This study of the 8 sand propose an approach to integrate all the available information in order to describe a reservoir characterized by important internal variability below the resolution of conventional tools. The principal steps of the study are summarized here:

- 1) Structural analysis of the field showing the preeminent role of salt in the constitution of trap and the presence of two major faults believed to be sealing.
- 2) Stratigraphic mapping of the reservoir revealed variations in thickness suggesting the location of the major flow-path and possible lateral stacking.
- 3) Thickness and net-to-gross estimation from using seismic data enabled to detect the lateral variation in the quality of the reservoir.
- 4) Lithofacies characterization from core showed that three facies could be used to describe the internal variability of the reservoir. These facies were defined by the average thickness of lamination and proportion of sand (Plantevin, 2002) and constituted the elements of the description of the internal variability of the reservoir.
- 5) The reservoir was simulated constrained by well and seismic. Seismic enable to account for large-scale lateral variation in facies proportions. Well information is used to model the vertical distribution of facies through vertical proportion curves.

This approach enabled to build a consistent reservoir model despite the poor spatial repartition of well data and the limited number of well. Lithofacies simulation enabled to represent the internal heterogeneity and will allow several parameters to be tested using flow simulation.

REFERENCES CITED

- Alabert, F.G., Massonnat, G. J., 1990, Heterogeneity in a complex turbiditic reservoir: stochastic modeling of facies and petrophysical variability: SPE paper 20604, presented at the 1990 SPE ATCE, New Orleans, 23-26 Sept.
- Alabert, F. G., Corre B., 1991, Heterogeneity in a complex turbiditic reservoir: impact on field development: SPE paper 22902, presented at the 1991 SPE ATCE, Dallas, 6-9 October.
- Armentrout, J. M., Malecek S.J., Mathur V.R. Neuder G.L, 1995, Meeting abstract: Intraslope basin reservoir deposited by gravity driven process: Ship Shoal and Ewing Bank areas (Offshore Louisiana): AAPG Bulletin, V.79, No 6, p. 905.
- Behrens, R.A., MacLeod M.K., Tran T.T., Alimi O., 1996, Incorporating seismic attribute maps in 3D reservoir models: SPE paper 36499 presented at the 1996 SPE ATCE, Denver, 6-9 October
- Beucher, H., Fournier F., Doligez B., Rozanski J., 1999, Using 3D seismic-derived information in lithofacies simulation. A case study: SPE paper 56736, presented at the 1999 SPE ATCE, Houston, 3-6 October.
- Bleines, C., Deraisme J., Geffroy F., Jeanne N., Perseval S., Rambert F., Renard D., Touffait Y., 2001, Isatis software manual, 3rd edition: Avon, France, Geovariances, 579 p.
- Bouma, A.H., Normark, W.R., Barnes, N.E., (eds.) , 1985, Submarine fans and related turbidite systems: New York, Springer Verlag, p. 319-324.
- Bouma, A.H., 2000, Fine grained, mud rich turbidite systems: model and comparison with coarse grained, sand rich systems *in* A.H. Bouma and C.G. Stone eds, Fine grained turbidite systems, AAPG memoir 72/SEPM Special publication 68, p. 9-20.
- Boyer, S., 1999, Well logging: Paris, Editions Technip. 192p.
- Bradshaw, B.E., Watkins J.S., 1996, Meeting abstract: Growth faults and growth-faults mechanisms observed in the Gulf of Mexico: AAPG V. 80, No. 9, p. 1495.

- Brinkmann, P. M. , Barbier, O. J., Rodriguez, W., 1987, Design and installation of a 20 slot template in the Gulf of Mexico by 760 ft of water: SPE paper 14579, presented at the 1985 Offshore Technology Conference, Houston, 6-9 May.
- Brown, A., 1999, Three-dimensional interpretation of seismic data: AAPG memoir 42, SEG investigation in geophysics No 9, 345 p.
- Burns, C. S., 1986, Relating Gulf coast sand/shale statistics to petrophysical properties as seen by seismic: SPE paper 15527 presented at the 1986 SPE ATCE, New Orleans, 5-8 October.
- Caers, J.K., Srinivasan S., Journel A.G., 2000, Geostatistical quantification of geological information for a fluvial type North Sea reservoir: SPE paper 56655 presented at the 1999 SPE ATCE, Houston 3-6 October
- Caers, J., Avseth P., Mukerji T., 2001, Geostatistical integration of rock physics, seismic amplitude and geological model in North Sea turbidite system: SPE paper 71321, presented at the 2001 SPE ATCE, New Orleans, Sept 30-October 3.
- Chen, Q., Sidney S., 1997, Seismic attribute technology for reservoir forecasting and monitoring: *The Leading Edge*, V. 16, No 5, p 445-509.
- Darling, H. R., Sneider R.M , 1992, Production of low resistivity, low contrast reservoirs, offshore Gulf of Mexico basin: *Gulf Coast Association of Geological Society Transactions*, abstract, v.42, p. 73-88.
- Doligez, B., Beucher H., Geffroy F., Eschard R., 1999, Integrated reservoir characterization: improvement in heterogeneous stochastic modeling by integration of additional constraints: *in* Schatzinger and J. Jordan eds, *Reservoir characterization recent advances*, AAPG memoir 71, p 333-342.
- Doyen, P.M., 1989, Porosity from seismic data: a geostatistical approach: SPE reprint series No. 27, *Reservoir Characterization V. 2*, p. 25-37.
- Doyen, P.M., den Boer L.D., Pillet W.R., 1996, Seismic porosity mapping in the ekofisk field using a new form of collocated cokriging: SPE paper 36498 presented at the 1996 SPE ATCE, Denver, 6-9 October
- Eschard, R., Lemouzy P., Desaubliaux G., Parpan J., Smart B., 1998, Combining sequence stratigraphy, geostatistical simulations and production data for modeling a

fluvial reservoir in the Chaunoy field (Triassic, France): AAPG Bulletin, V.82, No 4, p. 545-568.

- Fournier, F., Derain J.F., 1995, A statistical methodology for deriving reservoir properties from seismic data: Geophysics, V. 60, No 5, p 1437-1450
- Fugitt, D.S., Florstedt J.E., Herricks G.J., Wise M.R., Stelting C.E., Schweller W.J., 2000, Production characteristics of sheet and channelized turbidite reservoirs, Garden Banks 191, Gulf of Mexico: The Leading Edge, V. 19, No 4, p 356-369.
- Galli, A. Beucher H., 1997, Stochastic models for reservoir characterization: a user-friendly review: SPE paper 38999, presented at the fifth LACPEC, Rio de Janeiro, 30 August-3 September.
- Giudicelli, C.B., Massonnat G.J., Alabert F.G., 1992, Anguille Marine, a deepsea fan reservoir offshore Gabon: from geology toward history matching through stochastic modeling: SPE paper 25006, presented at the European Petroleum Conference in Cannes, France, 16-18 Nov.
- Haas, A., Dubrule O., 1999, Petroleum geostatistics, from the stone age to industrial times: *in* Proceedings of the 5th Annual Conference of the International Association for Mathematical Geology, Lippard, Naess and Sinding-Larsen eds, V 2, p 485-491.
- Haldorsen, H.H., Damsleth E, 1990, Stochastic modeling: JPT, (April 1990), p. 404-412.
- Handyside, D. D., Karaoguz O. K., Deskin R. H., Mattson G.A., 1992, A practical application of stochastic modeling techniques for turbidite reservoirs: SPE paper 24892, presented at the 1992 SPE ATCE, Washington, 4-7 October.
- Hansen, S. M., Fett T., 2000, Identification and evaluation of turbidite and other deepwater sands using open hole logs and borehole images: *in* A.H. Bouma and C.G. Stone eds, Fine grained turbidite systems, AAPG memoir 72/SEPM special publication 68, p. 317-338.
- Hohn, M.E., 1999, Geostatistics and petroleum geology: New York, Kluwer Academic Publishers. 235 p.

- Iledare, O. O., 2000, Trends in the effectiveness of petroleum exploration and development drilling in the U.S. Gulf of Mexico OCS region, 1977-1998: SPE paper 63060, presented at the 2000 SPE ATCE in Dallas, 1-4 October.
- Isaaks, E. H., Srivastava R.M., 1989, An introduction to applied geostatistics: New York, Oxford Univ. Press.
- Johann, P., Fournier F. Souza O., Eschard R., Beucher H., 1996, 3-D Stochastic reservoir modeling constrained by well and seismic data on a turbiditic field: SPE paper 3650, presented at the 1996 SPE ATCE, Denver, 6-9 October.
- Johann, P., de Castro D. D., Barroso A. S., 2001, Reservoir geophysics: seismic pattern recognition applied to ultra-deepwater oilfield in Campos Basin (offshore Brazil): SPE paper 69483, presented at the 2001 SPE LACPEC, Buenos Aires, 25-28 March.
- Jordan, D.L., Goggin D.J., 1995, An application of categorical indicator geostatistics for facies modeling in sand rich turbidite systems: SPE paper 30603, presented at the 1995 SPE ATCE, Dallas, 22-25 October.
- Journel, A., 1990, Geostatistics for reservoir characterization: SPE paper 20750, presented at the 1990 SPE ATCE, New Orleans, 23-26 Sept.
- Journel, A.G., Alabert F.G., 1990, Focusing on spatial connectivity of extreme-valued attributes: stochastic indicator models of reservoir heterogeneities: SPE paper 1989, presented at the 1988 SPE ATCE Houston, 2-5 October.
- Kalkomey, C.T., 1997, Potential risks when using seismic attributes as predictors of reservoir properties: *The Leading Edge*, V. 16, No 3, p 225-291.
- Karlo, J.F., Shoup R. C., 2000, Classification of syndepositional systems and tectonic provinces of the Northern Gulf of Mexico, adaptation for online presentation from poster session at Houston Geological Society Dinner Meeting, February 7, 2000; <www.searchanddiscovery.com/documents/karlo.index.htm>, accessed January 2002.
- Khan, A., Horowitz D., Liesch A., Schepel K., 1996, Semi-amalgamated thinly-bedded deepwater GOM turbidite reservoir performance modeled using object-based technology and Bouma lithofacies: SPE paper 36724, presented at the 1996 SPE ATCE, Denver, 6-9 October.

- Kumins, L., 2000, IB 1005: Outer continental shelf: oil and gas leasing and revenue, <<http://www.cnie.org/nle/eng-45.html>>, accessed January 7, 2002.
- Mann, R.G., Bryant W.R., Rabinowitz P. D., 1987, Seismic stratigraphy and salt tectonic of the Northern Green Canyon area, Gulf of Mexico: Technical report 87-5-T, November 1987, Department of Oceanography, Texas A&M University.
- Matheron, G., Beucher H., Galli A., Guerillot D., Ravenne C., 1987, Conditional simulation of the geometry of fluvio-deltaic reservoirs: SPE paper 16753, presented at the 1987 SPE ATCE, Dallas, 27-30 September.
- Mc Bride, B.C., Weimer P., Rowan M.G., 1998, The effect of allochthonous salt on the petroleum systems of Northern Green Canyon and Ewing Bank (offshore Louisiana), Northern Gulf of Mexico: AAPG Bulletin, V.82, No 5B, p. 1083-1112.
- Mitchum, R. M., Sangree, J. B., Vail P. R., Wornardt W.W., 1993, Recognizing sequences and systems tracts from well logs, seismic data, and biostratigraphy: examples from the late Cenozoic of the Gulf of Mexico: M 58, Siliciclastic Sequence Stratigraphy: Recent Developments and Applications, AAPG Special Publication, p 163-197.
- Mutti, E., Normark W.R., 1987, Comparing examples of modern and ancient Turbidite systems: Problem and concepts: *in* Leggett, J.K., and Zuffa, G.G. (eds): Marine clastic sedimentology; concepts and case studies, London, Graham and Trotman, p.1-38.
- Norris, R. J., Massonnat G. J., Alabert F. G., 1993, Early quantification of uncertainty in the estimation of oil in place in a turbidite reservoir: SPE paper 26490, presented at the 1993 SPE ATCE, Houston, 3-6 October
- Pacht, J. A., Bowen, B. E., 1990, Abstract: Sequence stratigraphy along an unstable progradational continental margin Pliocene-Pleistocene (Offshore Louisiana): AAPG Bulletin , V. 74, No 5, p 735 - 735
- Pickering, K.T., Ricci Lucchi, F., Smith, R., Kenyon, N.H., Hiscott, R.N., & Clark, J.D., 1995, Introduction: Architectural element analysis of turbidite systems: *in* Pickering, K.T., Ricci Lucchi, F., Smith, R., Hiscott, R.N., & Kenyon, N.H., eds., An atlas of deep-water systems: London, Chapman and Hall, p.1-10.

- Plantevin, M., 2002, Characterization of the 3-D properties of the fine-grained turbidite 8 sand reservoir, Green Canyon 18, Gulf of Mexico: M.S. Thesis, Geology and Geophysics, Texas A&M University.
- Prather, B.E., Booth J. R., Steffens G.S., Craig P.A., 1998, Classification, lithologic calibration and stratigraphic succession of seismic facies of intraslope basins, deep-water Gulf of Mexico: AAPG Bulletin, V.82, No 5a, p701-728.
- Ravenne, C., Beucher H., 1988, Recent development in description of sedimentary bodies in a fluvio deltaic reservoir and their 3D conditional simulations: SPE paper 18310, presented at the 1988 SPE ATCE, Houston 2-6 October.
- Reading, H.G., Richards M., 1994, Turbidite systems in deep-water basin margins by grain size and feeder system. AAPG Bulletin, V. 78, No. 5, pp.792-822.
- Scheibal, J. R., Weiland J. L., Worrel J. M., 1992, An integrated subsurface study directed at optimizing turbidite sand completion strategies: SPE paper 24725, presented at the 1992 SPE ATCE, Washington DC, 4-7 October.
- Schultz, P. S., Hattori M., Mantran P., Hoskins J., Corbett C., 1994, Seismic guided estimation of rock properties: SPE paper 28386, presented in the ATCE, New Orleans, 25-28 September.
- Shew, R. D., Tiller G.M., Hackbarth C.J., Rollin D.R., White C. D., 1995, Characterization and modelling of channel and thin-bedded turbidite prospect in the Gulf of Mexico: integration of outcrops, modern analogs and subsurface data: SPE paper 30535, presented at the 1995 SPE ATCE, Dallas, 22-25 October.
- Shmaryan, L.E., Deutsch C.V., 1999, Object-based modeling of fluvial/deepwater reservoirs with fast data conditioning: methodology and case studies: SPE paper 56821, presented at the 1999 SPE ATCE, Houston 3-6 October.
- Srivastava, R.M., 1994, An overview of stochastic methods for reservoir characterization: *in* AAPG special publication CA 3: Stochastic Modeling and Geostatistics Edited by Jeffrey M. Yarus and Richard L. Chambers, p.3-16.
- Suro-Prerez, V., Ballin P., Aziz K., Journel A.G., 1991, Modeling geological heterogeneities and its impact on flow simulation: SPE paper 22695, presented at the 1991 SPE ATCE, Dallas, 6-9 October

- Taner, M.T., 1979, Seismic trace attributes and their projected use in prediction of rock properties and seismic facies < www.rocksolidimage.com>, accessed January 2001.
- Varnai, P., 1998, Three-dimensional seismic stratigraphic expression of Pliocene-Pleistocene turbidite systems, Northern Green Canyon, Northern Gulf of Mexico: AAPG Bulletin, V.82, No 5B, p. 986-1012.
- Weber, K. J., van Geuns L. C., 1990, Framework for constructing clastic reservoir simulation models: SPE paper 19582, presented at the 1989 SPE ATCE, Sam Antonio, Texas, 8-11 October.
- Weimer, P., Crews, J.R., Crow, R. S., Varnai, P., 1998a, Atlas of petroleum fields and discoveries, Northern Green Canon, Ewing Bank, and Southern Ship Shoal and South Trimbaler areas (offshore Louisiana), Northern Gulf of Mexico: AAPG Bulletin, V.82, No 5B, p. 878-917.
- Weimer, P., Rowan M. G., Mc Bride B. C., Kligfield R., 1998b, Evaluating the petroleum systems of the northern deep Gulf of Mexico through integrated basin analysis: an overview: AAPG Bulletin, V.82, No 5B, p. 865-877
- Weimer, P., Varnai P., Budhijanto F. M., Acosta Z. M., Martinez R. E., Arango C., Crew J. R., Pulham A. J., 1998c, Sequence stratigraphy of Pliocene and Pleisocene Turbidite systems, Northern Green Canyon and Ewing Bank (offshore Louisiana), Northern Gulf of Mexico: AAPG Bulletin, V.82, No 5B, p. 918-960.
- Weimer, P., Roger M. S., 1999, Turbidite systems, part 1: Sequence and seismic stratigraphy: The Leading Edge, V. 18, No 4, p 454-462.
- Weimer, P., Slatt R.M., Dromgoole P., Bowman M., Leonard A., 2000, Developing and managing turbidite reservoirs: case histories and experiences: Results of the 1998 EAGE/AAPG research conference: AAPG Bulletin, V. 84, No 4, p 453-465.
- Xu, W., Tran T.T., Srivastava R.M. Journal A.G., 1992, Integrating seismic data in reservoir modeling: the collocated cokriging alternative: SPE paper 24742, presented at the 1992 SPE ATCE, Washington DC, 4-7 October.
- Zhang, H., 1994, Salt tectonics and sequence stratigraphy of central offshore Louisiana, Gulf of Mexico: PhD Dissertation Oceanography, Texas A&M University.

VITA

Séverine Lalande was born on November 11th 1977 in Guérande, France. She received a B. S. in engineering majoring in Earth Sciences from the Ecole Nationale Supérieure des Mines de Paris in July 2000. She entered the joint program “Reservoir Geoscience and Engineering” between Texas A&M and the French Institute of Petroleum in August 2000. Her permanent address is Les Pavillons, 44500 La Baule France.